Ciglitazone negatively regulates CXCL1 signaling through MITF to suppress melanoma growth

Thomas Botton, Alexandre Puissant, Yann Cheli, Tijana Tomic, Sandy Giuliano, Lluis Fajas, Marcel Deckert, Jean-Paul Ortonne, Corine Bertololotto, Sophie Tartare-Deckert, et al.

Ciglitazone negatively regulates CXCL1 signaling through MITF to suppress melanoma growth

Thomas Botton[1,2], Alexandre Puissant[1,2], Yann Cheli[1,2], Tijana Tomic[1,2], Sandy Giuliano[1,2], Lluis Fajas[3], Marcel Deckert[4], Jean-Paul Ortonne[1,2,5], Corine Bertolotto[1,2,5], Sophie Tartare-Deckert[1,2,5], Robert Ballotti[1,2,5] and Stéphane Rocchi[1,2,5].

1 INSERM, U895, équipe 1 Nice, France; 2 Université de Nice Sophia Antipolis, UFR de Médecine, IFR50, Nice, France; 3 Metabolism and Cancer Laboratory, CRLC Val d'Aurelle, Montpellier, France; 4 INSERM U576, Nice, France ; 5 Service de Dermatologie, CHU Nice, France

Address correspondence to: Stéphane Rocchi, INSERM U895, Centre Méditerranéen de Médecine Moléculaire (C3M), Bâtiment Archimed, 151 route de Saint Antoine de Ginestière, BP 2 3194, 06204 Nice cedex 3, France, Tel: (33) 4 93 37 76 99, Fax: (33) 4 89 06 42 21, srocchi@unice.fr

Running Title: Negative regulation of MITF/CXCL1 axis by ciglitazone

Abstract

We have previously demonstrated that the thiazolidinedione ciglitazone inhibited, independently of PPARγ activation, melanoma cell growth. Further investigations now show that ciglitazone effects are mediated through the regulation of secreted factors. Q-PCR screening of several genes involved in melanoma biology reveals that ciglitazone inhibits expression of the *CXCL1* chemokine gene. CXCL1 is overexpressed in melanoma and contributes to tumorigenicity. We show that ciglitazone induces a diminution of CXCL1 level in different human melanoma cell lines. This effect is mediated by the down regulation of microphthalmia-associated transcription factor, MITF, the master gene in melanocyte differentiation and involved in melanoma development. Further, recombinant CXCL1 protein is sufficient to abrogate thiazolidinedione effects such as apoptosis induction, while extinction of the CXCL1 pathway mimics phenotypic changes observed in response to ciglitazone. Finally, inhibition of human melanoma tumor development in nude mice treated with ciglitazone is associated with a strong decrease in MITF and CXCL1 levels.

Our results demonstrate that anti-melanoma effects of thiazolidinediones involve an inhibition of the MITF/CXCL1 axis and highlight the key role of this specific pathway in melanoma malignancy. (178 words)

Keywords: melanoma, thiazolidinedione, chemokine, MITF, apoptosis.

Introduction

Cutaneous melanoma is an aggressive skin cancer that originates from epidermal melanocytes. Typically, primary lesions progress to malignant tumors through a multistep process including dysplasia, radial growth phase (RGP), invasive vertical growth phase (VGP), and metastasis. This transition is accomplished through the accumulation of genetic alterations in growth control pathways including oncogenic mutations or gene amplification. For example, constitutive activation of the Ras/MAPkinase-signaling pathway is frequently observed in melanomas, as a consequence of activating mutations of the B-Raf and N-Ras genes [1-3]. Melanoma progression is also accompanied by generation of autocrine and paracrine loops associated with the aberrant production and secretion of growth factors and chemokines that sustain growth, survival and invasion [4].

In human, melanoma is one of the most lethal cancers among young adults. Melanoma has a high capability of invasion and rapid metastasis to other organs. The prognosis of metastatic melanoma is extremely dismal, as the various treatments have not shown survival benefit [5]. It appears thus necessary to develop approaches enabling the discovery of new molecular targets, candidates for specific biotherapy treatment of this disease.

Thiazolidinediones (TZD) regulate transcriptional activity of the nuclear receptor Peroxysome Proliferator Activated Receptor gamma (PPARγ) and are currently used in type II diabetes treatment. More recently, TZD have been reported to inhibit proliferation and survival of numerous cancer cells [6-11]. Furthermore, we have previously demonstrated that ciglitazone, that belongs to TZD family, inhibits growth and viability of melanoma cells without affecting normal melanocyte growth [12].

To further investigate the molecular events elicited by ciglitazone and to better understand the implication of TZD signaling in melanoma biology, we examined whether ciglitazone affects the production of autocrine and paracrine factors known to be implicated in melanoma

malignancy. In the present report, we demonstrate that ciglitazone inhibits the expression of (C-X-C motif) ligand 1 (CXCL1), a chemokine involved in melanoma growth, survival, angiogenesis and metastasis [13-16]. Interestingly, ciglitazone treatment decreases CXCL1 level in various human melanoma cell lines but not in normal human melanocytes. We also show that treatment of melanoma cells with recombinant CXCL1 compensates for the loss of endogenous CXCL1 secretion induced by ciglitazone and abolishes the loss of viability of melanoma cells. Further, CXCL1 inhibition by ciglitazone is mediated by the decrease in MITF expression. CXCL1 appears to be a new target gene of microphthalmia-associated transcription factor (MITF), the master gene of melanocyte differentiation that was also involved in melanoma development [17-21]. Finally, we demonstrate that a dramatic inhibition of melanoma xenograft development in mice in response to ciglitazone is associated with a decrease in MITF gene expression and in circulating CXCL1 level.

Our results demonstrate for the first time that ciglitazone-induced apoptosis of melanoma involves an inhibition of a MITF/CXCL1 signaling cascade.

Results

Effect of ciglitazone on CXCL1 expression and secretion

We first determined whether the biological effects of ciglitazone in melanoma cells were mediated by secreted factors. We confirmed that ciglitazone did not affect normal human melanocytes (NHM) viability (Fig. 1A).

In contrast, the number of melanocytes was significantly reduced when incubated in presence of conditioned medium from A375 melanoma cells exposed to ciglitazone compared to conditioned medium from DMSO-treated A375 cells (Fig. 1B). These results suggest that the inhibition of melanoma cells growth or survival elicited by ciglitazone was at least in part mediated by secreted factors.

To substantiate this observation, we analyzed by quantitative-PCR, the expression of 19 transcripts encoding for proteins known to be secreted by melanoma (Table 1). Among them ciglitazone clearly repressed the expression of *CXCL1*. Due to the important role of the CXCL1 chemokine in melanoma progression, we decided to investigate thoroughly the involvement of this cytokine in the effect of ciglitazone on melanoma cells.

RT-QPCR analysis confirmed a dose-dependent downregulation of *CXCL1* expression in ciglitazone-treated A375 melanoma cells (Fig. 2A). Then, we demonstrated a decrease in CXCL1 cytoplasmic protein by immunofluorescence (Fig. 2B). TNFα, an activator of NF-κB pathway, significantly increased CXCL1 level. To confirm the presence of CXCL1 receptor, CXCR2 labeling was carried out (Fig. 2B, lower part). A375 cells expressed CXCR2 receptor and ciglitazone did not change its expression.

CXCL1 amount in medium was evaluated by ELISA. TNFα increased CXCL1 level while ciglitazone induced a dose-dependent reduction of CXCL1 in both basal and TNFα conditions (Fig. 2C). Western blot of the secreted matricellular SPARC protein was used as loading control.

Relationship between CXCL1 downregulation and cell viability inhibition induced by ciglitazone

One could think that the inhibition of CXCL1 is the consequence of the decrease in cell viability induced by ciglitazone. However, reduction of CXCL1 was detectable after 2h and therefore could not result from the decrease in viability of cells that was observed after 12h (Fig. 3A). In contrast, the slight decrease in CXCL1 level observed after 12h to 48h of staurosporine treatment appeared to be the consequence of cell death induced by this agent.

Next, other TZD, pioglitazone and rosiglitazone had no significant effect on CXCL1 secretion (Fig. 3B). In contrast, troglitazone showed a dose-dependent decrease in CXCL1 level comparable to that observed with ciglitazone. Moreover, the decrease in CXCL1 level in response to ciglitazone treatment was still observable when PPARγ expression was abrogated by siRNA silencing, indicating that ciglitazone acts independently of PPARγ to repress CXCL1 expression (Fig. S1)

Interestingly, no CXCL1 was detectable in NHM (Fig. 3C). However, treatment of melanocytes by TNFα induced an increase in the level of CXCL1 that was not modulated by ciglitazone. Ciglitazone was unable to control CXCL1 expression in melanocytes.

Finally, we tested ciglitazone on different tumor cell lines. SK-Mel-28, WM793 and 1205 Lu melanoma cells had basal CXCL1 levels comparable to that found in A375 while MeWo had very low CXCL1 level. In all melanoma cells, TNFα induced a significant increase in CXCL1 level and ciglitazone decreased strongly the chemokine level. In contrast to neuroblastoma cells SH-SY5Y, prostate tumor cells PC-3 presented a high CXCL1 basal level. As in melanoma cells, TNFα significantly increased the cytokine level in both cell lines while ciglitazone strongly reduced CXCL1 level (Fig. 3D). The effects of ciglitazone on growth and survival in these cell lines were tested (Fig. 3E and S2). Ciglitazone treatment decreased cell

number in all tumor cell lines tested so far. However, the most striking effect was observed in melanoma cell lines with a high basal CXCL1 level.

Effect of recombinant CXCL1 on the decrease in cell viability induced by ciglitazone

To determine whether CXCL1 inhibition played an important role in ciglitazone-induced loss of melanoma cell viability, we compensated the loss of endogenous CXCL1 by adding human recombinant CXCL1 (rCXCL1). As expected, ciglitazone (10µM) induced a loss of 65% of cell viability (Fig. 4A). Addition of rCXCL1 prevented in a dose-dependent manner the loss of cell viability. Similarly, the reduction of cell viability induced by ciglitazone was reversed by TNFα (Fig. 4B). Consequently, rCXCL1 as well as the TNFα-induced CXCL1 increase induced by TNFα had a protective effect against ciglitazone action.

Interestingly, rCXCL1 did not prevent cell viability reduction mediated by two apoptosis inductors, TRAIL and staurosporine (Fig. 4C). The protective effect of rCXCL1 thus seems specific of the ciglitazone action.

We have previously established that low concentrations of ciglitazone induced a G0/G1 cell cycle arrest of A375 melanoma cells. Our results demonstrated that rCXCL1 was able to reverse ciglitazone-induced cell cycle arrest (Fig. S3).

We have also shown that high concentrations of ciglitazone induced melanoma cells apoptosis. We observed that 10µM ciglitazone induced the disappearance of the zymogenic form of caspases 3, 8 and 9 as well as a cleavage of poly(ADP-ribose) polymerase (PARP). Consistently with the protective effect of rCXCL1, cleavage of caspases and PARP evoked by 10µM ciglitazone were not detected in presence of rCXCL1 (Fig. 5A). These results were confirmed by caspase 3, 8 and 9 activation assays (Fig. 5B). Interestingly, rCXCL1 was not able to prevent the activation of these three caspases induced by staurosporine. Further, flow cytometry analysis showed that rCXCL1 blocked the accumulation of cell in sub-G1 (Fig. S3)

and prevented the increase in annexin-V labeling (Fig. 5C), both induced by ciglitazone. In conclusion, CXCL1 protects melanoma cells from apoptosis induced by ciglitazone.

Our observations prompted us to check whether CXCL1 inhibition was sufficient to reduce melanoma cell viability. Transfection of A375 cells with increasing concentrations of si-CXCL1 induced a strong and dose dependent reduction of the CXCL1 protein level (Fig. 6A). Using XTT assay, we observed that A375 cells transfected with si-CXCL1 showed a dose-dependent reduction of cell viability reaching 50% decrease at 50 nM of si-CXCL1 (Fig. 6B). Addition of rCXCL1 completely restored the cell viability. Then, we observed a dose-dependent reduction of A375 cell viability in the presence of anti-CXCL1 neutralizing antibodies (Fig. 6C). No significant reduction in the viability of these cells was detected in presence of control antibodies.

We next showed that CXCL1 silencing induced the activation of caspases 9, 8 and 3 (Fig. 6D) as well as an increase in annexin-V labeling (Fig. 6E). Taken together, these results indicate that the inhibition of CXCL1 production is sufficient to induce apoptosis in melanoma cells. In the same way, inhibition of CXCR2 signaling by neutralizing antibody or pharmacological inhibitor (SB225002) mimics the effects of ciglitazone on growth inhibition (Fig. S4).

Involvement of MITF in the regulation of CXCL1 expression by ciglitazone

To further investigate the mechanism responsible for ciglitazone-induced CXCL1 downregulation, we focused our attention on MITF that was recently reported to be regulated by some PPARγ agonists [22,23]. Ciglitazone induced a dose-dependent reduction of MITF expression in both A375 and SK-Mel-28 melanoma cells (Fig. 7A). We demonstrated that MITF inhibition by ciglitazone was not due to its cleavage during apoptosis since the MITF decrease was observed after 2h of treatment, while PARP cleavage appeared clearly later (12h). To confirm this result we showed that the pan-caspase inhibitor Z-VAD-FMK

prevented melanoma cell death induced by ciglitazone treatment (Fig. S5) by preventing apoptosis induction monitored by PARP processing (Fig. 7A, Right panel). However, MITF inhibition evoked by ciglitazone was still observed in the presence of Z-VAD-FMK. Finally, using RT-QPCR, we also found a dose-dependent decrease of *MITF* expression confirming that ciglitazone inhibited MITF expression at the transcriptional level (Fig. 7B).

We next checked whether MITF might control CXCL1 expression. MITF silencing by specific si-RNA induced a strong reduction of the *MITF* transcript and a concomitant reduction of *CXCL1* gene expression (Fig. 7C). Melanoma cells transfected with a vector encoding for wild-type MITF revealed an increased in CXCL1 labeling by immunofluorescence (Fig. 7D). Consistently, forskolin or forskolin/IBMX that increased endogenous MITF level showed a significant increase in CXCL1 (Fig. 7E).

To determine whether MITF controlled the CXCL1 promoter activity, we performed luciferase assays on melanoma cells using either tyrosinase or CXCL1 promoter upstream the luciferase coding sequence. Transfection with a dominant negative form of MITF (DN MITF) led to a decrease in both tyrosinase and CXCL1 promoter activity. The effect on CXCL1 promoter was weak but significant. Conversely, transfection of A375 melanoma cells with the wild-type form of MITF (MITF) led to an upregulation of tyrosinase and CXCL1 promoter activity (Fig. 7F).

Then, to verify the binding of MITF to the CXCL1 promoter in intact cells, we performed chromatin immunoprecipitation (ChIP) assays. Direct PCR amplification with specific primers spanning the CXCL1 promoter between -410 and +77, on total DNA extract or after immunoprecipitation with antibody to polymerase II as a positive control amplified a 500bp fragment (Fig. 7G). Alternatively, after immunoprecipitated with non-immune mouse IgG no amplification could be observed. After immunoprecipitation with anti-MITF, we amplified a band at 500bp corresponding to the CXCL1 promoter. The intensity of this band was clearly

decreased in extracts from cells exposed to ciglitazone but not in extracts from cells exposed to forskolin (Fsk). Conversely, using specific GAPDH promoter primers, we amplified 160bp-fragment corresponding to the GAPDH promoter in both the total extract and the anti-Pol II precipitates, but not in the anti-MITF precipitates. These results demonstrate that MITF binds to the CXCL1 promoter in intact cells and that this interaction is abolished by ciglitazone treatment.

Effect of ciglitazone on circulating CXCL1 and melanoma tumor xenografts development in mice.

Then, to determine the effect of ciglitazone on circulating CXCL1 and on tumor development *in vivo*, human A375 melanoma cells were injected subcutaneously in athymic nude mice. Nineteen days post injection, mice were treated with vehicle or ciglitazone (50mg/kg/day) during 11 days.

Tumors from untreated mice dramatically grew throughout the time course of the study (Fig. 8A). In contrast, treatment of mice with ciglitazone markedly attenuated the capacity of cells to develop visible tumors. Indeed, 3 out of 6 ciglitazone treated-mice did not have a measurable tumor at the end of the treatment. Moreover, visible tumors of other mice were significantly smaller compared to untreated control mice confirming that ciglitazone has anti-melanoma activity *in vivo*.

After mice sacrifice, RT-QPCR were performed on RNA extracted from tumors. Interestingly, MITF and CXCL1 gene expression were significantly lower in tumors of mice treated with ciglitazone (Fig. 8B). In parallel, we measured the quantity of serum CXCL1 (Fig. 8C). A huge amount of circulating CXCL1 was detected in mice with human melanoma tumors compared to non-tumor bearing mice (no detectable human CXCL1). Further, no significant CXCL1 level was detected in mice treated with ciglitazone in comparison to

vehicle-treated mice. When we expressed the quantity of serum CXCL1 as a function of tumor volume, we observed a 3.5-fold significant reduction in the level of circulating CXCL1 in ciglitazone-treated mice. Therefore, the decrease in CXCL1 serum level observed in ciglitazone-treated mice was not due to a decrease in tumor volume, but was likely a consequence of CXCL1 inhibition induced by ciglitazone. Finally, to unequivocally demonstrate the importance of CXCL1 downregulation in the *in vivo* effects of ciglitazone, we evaluated the effects of rCXCL1 peritumoral injections (200 ng/tumor/day for 14 days) on the development of tumors in mice treated or not with ciglitazone. As expected, treatment of mice with ciglitazone markedly impaired tumors development (Fig. 8D). However, rCXCL1 treatment dramatically favored tumor development and abrogated anti-tumoral effects of ciglitazone. Injection of human recombinant CXCL1 therefore compensates for the decrease in endogenous CXCL1 level mediated by ciglitazone treatment and promotes tumor growth. This experiment clearly demonstrates the importance of CXCL1 expression in melanoma tumor development and highlight the pivotal role of CXCL1 downregulation in ciglitazone effects.

Discussion

Because metastatic melanoma are resistant to all currently used treatments, the discovery of new therapeutic drugs is a very important challenge. We and others have previously shown that ciglitazone, a molecule of the TZD family, is able to induce apoptosis independently of PPARγ activation and to inhibit proliferation of melanoma cells [12,24-26]. In the present report, we have investigated the molecular mechanism by which ciglitazone exerts its anti-melanoma activity.

Our results showed that conditioned media from ciglitazone-treated melanoma cells inhibit normal human melanocyte growth indicating that the effects of ciglitazone on melanoma cells are mediated by secreted factors. RT-QPCR screening demonstrating an inhibition of CXCL1 chemokine upon ciglitazone treatment prompted us to focus our attention on this cytokine. CXCL1, also named Melanoma Growth Stimulating Activity (MGSA) or Growth Regulated Oncogene alpha (GROα) belongs to the CXC family. CXCL1 is essential for the establishment and the maintenance of the tumoral potential of melanoma [27,28]. The CXCL1 gene product is located within the *CXCL1-3* gene cluster on chromosome *4q12-q13* [29]. CXCL1, CXCL2 and CXCL3 bind with high affinity to a common receptor, CXCR2, with CXCL1 having the highest affinity for this receptor [30]. Overexpression of CXCL1 in INK4a/ARF$^{-/-}$ mice favors melanoma development [31] and promotes malignant growth of murine squamous cell carcinoma by a CXCR2 dependent pathway [32]. Blocking antibodies to either CXCL1 or CXCR2 inhibit melanoma cell growth demonstrating the key role of the CXCL1/CXCR2 signaling pathway in melanoma development [33,34]. In addition to its autocrine role, CXCL1 has been shown to play an important paracrine role by regulating angiogenesis during tumor development including melanoma [35,36].

First, we demonstrate that ciglitazone negatively regulates mRNA and protein CXCL1 levels. This inhibition is accompanied by a reduction of CXCL1 in the medium. The inhibition of

CXCL1 in response to ciglitazone precedes the decrease in cell viability, indicating that the decrease in CXCL1 expression induced by ciglitazone is not a consequence of cell death. A similar decrease in CXCL1 is also observed in response to troglitazone while rosiglitazone and pioglitazone have no significant effect on CXCL1 secretion. This result is in agreement with our previous report demonstrating that both rosiglitazone and pioglitazone have only marginal PPARγ dependent effect on viability of melanoma cells [12]. Consistent with this finding, PPARγ silencing by siRNA does not abrogate the effects of ciglitazone on CXCL1 expression, indicating that the regulation of CXCL1 is PPARγ independent.

In normal human melanocytes, there is not basal CXCL1 production. Treatment of normal human melanocytes with TNFα stimulation increases CXCL1 secretion that is not affected by ciglitazone. Conversely, melanoma cells generally have a constitutive basal CXCL1 expression mainly due to the NF-κB pathway constitutive activation [27]. Independently of the mutational status, melanoma development stage or CXCL1 basal level, we found that ciglitazone inhibits CXCL1 production in all tested melanoma cell lines. Moreover, there is a positive correlation between the level of basal CXCL1 and the decrease in cell viability mediated by ciglitazone, suggesting that melanoma cells producing CXCL1 are addict to these cytokine.

In the same way, in other cancer cell lines such as prostate carcinoma or neuroblastoma, ciglitazone also decreases CXCL1 level and cell viability. These results support the idea that inhibition of CXCL1 cytokine could play a general role in the anti-tumoral effects of ciglitazone.

It has been proposed that some PPARγ agonists lead to inhibition of NF-κB activation [37-39], but in our system, the inhibition of CXCL1 by ciglitazone is not mediated by the down-regulation of NF-κB activity (data not shown). Interestingly, a recent paper showed that ciglitazone led to a decrease in MITF expression [22] and *in silico* analysis of the CXCL1

promoter showed four potential E boxes that match with the consensus binding-site for MITF transcription factor (data not shown), thereby suggesting the possible involvement of MITF in the control of *CXCL1* expression. These two observations promoted us to investigate the role of MITF in the regulation of CXCL1 by ciglitazone. First, ChIP experiments and luciferase assays demonstrate that MITF binds to and regulates the *CXCL1* promoter. MITF silencing decreases *CXCL1* messengers and inhibits CXCL1 protein secretion. Additional studies suggest that MITF interacts with the *CXCL1* promoter through a responsive element (CAGGTG) at -375.

Further, we have previously found that MITF is cleaved in response to the apoptosis inductor, TRAIL [40]. MITF diminution that we observed in response to ciglitazone is not due to a protein cleavage by caspases since MITF decrease is seen before apoptosis induction and is also seen on mRNA level and in presence of pan-caspase inhibitor Z-VAD-FMK. These interesting results highlight a new specific pathway mediated by ciglitazone in melanoma cells. We have demonstrated that the negative regulation of MITF by ciglitazone is a PPARγ independent event. However, the precise mechanism responsible for this negative regulation of MITF is not known. One possible mechanism might involve downregulation of the Wnt/β-catenin pathway because this pathway is inhibited by some PPARγ agonists and might mediate the inhibition of MITF expression [22,23]. Thus, considering all our results we demonstrate for the first time that the control of MITF expression by ciglitazone is involved in the inhibition of CXCL1 expression and secretion. This new signaling pathway involves MITF in the regulation of CXCL1 and strengthens the importance of this transcription factor in melanoma tumorigenicity.

We have previously demonstrated that ciglitazone has cytostatic and cytotoxic effects [12]. We found that both cell cycle arrest and apoptosis evoked by ciglitazone are reversed by addition of rCXCL1 or TNFα. These data suggest that ciglitazone effects on cell viability are mediated

mainly by a decrease in CXCL1 expression and secretion. In addition, rCXCL1 does not protect cells from apoptosis induced by TRAIL and staurosporine, suggesting a potential specificity of rCXCL1 on ciglitazone effects. The depletion of CXCL1 with siRNA is sufficient to mimic the biological effects of ciglitazone on A375 cells. Consequently, these results reinforce the hypothesis that inhibition of CXCL1 synthesis by ciglitazone is implied in the biological effects of this TZD. A second approach by CXCL1 neutralizing antibodies confirmed these results. Therefore, the reduction of secreted form of CXCL1 is involved in ciglitazone biological effects.

At the molecular level, the stimulation of CXCR2 by CXCL1 induces activation of several transduction pathways, and particularly Raf/MEK/ERK and PI3K/Akt pathways [14]. However, in most melanoma cells, Raf/MEK/ERK pathway is constitutively active due to oncogenic mutation on B-Raf [41]. Consequently, this cytokine rather exerts its action on proliferation/survival through the activation of the PI3K/Akt pathway.

Finally, we have evaluated the correlation between potential anti-melanoma activity of ciglitazone and CXCL1 secretion in a mouse model of melanoma xenografts. We have previously demonstrated that ciglitazone prevents tumor growth development [12]. Importantly, our present results show that the short-term administration of ciglitazone not only prevents tumor formation but also reduces the volume of already established melanoma tumors. In addition, ciglitazone decreases *MITF* and *CXCL1* mRNA level in tumor xenograft, reinforcing the hypothesis that *in vivo*, MITF is also involved in the control of CXCL1 mediated by ciglitazone. In parallel, we observe a drastic reduction of serum CXCL1 level in mice. This decrease is not due to the reduction of tumor growth because when we expressed the quantity of CXCL1 as a function of tumor size, we still found a reduction of circulating CXCL1 in ciglitazone-treated mice. Moreover, injection of CXCL1 in ciglitazone treated mice compensates for the loss of endogenous CXCL1, impairing the effects of ciglitazone and

preventing the decrease in tumor volume. From these observations, we can propose that the decrease in CXCL1 secretion mediated by ciglitazone might be responsible for the antineoplastic effects of this TZD *in vivo*.

In summary, we demonstrate for the first time that ciglitazone inhibits tumor growth through a negative regulation of the MITF/CXCL1/CXCR2 axis signaling pathway. This demonstration brings new and additional clues to the mechanism of ciglitazone-induced melanoma cell death. Finally, taking into account the drastic effect of ciglitazone on melanoma cell growth, survival and anti-melanoma xenograft development, it might be worth evaluating ciglitazone treatment in patients with metastatic melanoma. Our reports also highlight the pivotal role of tumor cell-produced CXCL1 in melanoma cell proliferation and support the idea that CXCL1 might be used as a new progression marker in the follow-up of the metastatic melanomas. Because the overexpression of CXCL1 and the CXCL1-regulation by ciglitazone are not specific to the melanomas, our study, besides its interest in melanoma pathology, contributes to better understand the general anti-cancer effects of ciglitazone.

Material and methods

Materials

Ciglitazone, Troglitazone and Z-VAD-FMK were purchased from Biomol (Tebu, Le Perray en Yvelines, France). Pioglitazone and Rosiglitazone were from Cayman Chemical Company (Ann Arbor, MI, USA). Dimethyl sulfoxide (*DMSO*), staurosporine, forskolin, 3-Isobutyl-1-methylxanthine (IBMX), hydrocortisone, insulin, phorbol-12 myristate 13-acetate, MCDB 153 medium, sodium fluoride, dimethylacetamide, Hoechst 33258, tween 80, sodium orthovanadate, 4-(2-aminoethyl)-benzene-sulfonyl fluoride (AEBSF), aprotinin and leupeptin were purchased from Sigma-Aldrich (Saint Quentin Fallavier, France). Labrafil M 1944 Cs was purchased from Gattefossé (Saint-Priest, France). The caspase substrates and the caspase inhibitors were from MERCK Eurolab (Fontenay-sous-Bois, France). Trypan blue, Dulbecco's Modified Eagle's Medium (DMEM), penicillin/streptomycin and trypsin were from Invitrogen (Pontoise, France); Fetal Calf Serum (FCS) from Hyclone (Brevieres, France). TRAIL was obtained from R&D Systems (Lille, France). Recombinant human TNFα and recombinant human CXCL1 were purchased from Peprotech (Neuilly-sur-Seine, France).

Cell cultures

Normal human melanocytes were prepared and maintained as described [42]. Human A375 (CRL-1619^{TM}), SK-Mel-28 (HTB-72^{TM}) and MeWo (HTB-65^{TM}) melanoma cells, prostate cancer PC-3 (CRL-1435^{TM}) and neuroblastoma SH-SY5Y (CRL-2266^{TM}) cell lines were purchased from American Tissue Culture Collection (Molsheim, France) and grown in DMEM medium supplemented with 10% FCS and penicillin/streptomycin (100U/ml/50 µg/ml). Human WM793 vertical growth phase melanoma cell line and 1205 Lu metastatic melanoma cell line were generously provided by Dr M. Herlyn (Wistar Institute, Philadelphia, PA) and maintained as described [43]. For each experiment, cells were starved in appropriate medium without FCS during 14 hours before drug stimulation.

Antibodies.

HSP60 was from Santa Cruz Biotechnology (TEBU; Le Perray en Yvelines, France). The polyclonal pro-caspase 9, monoclonal pro-caspase 8, monoclonal pro-caspase 3 and polyclonal PARP antibodies were from Cell Signaling Technology (Ozyme, Saint-Quentin-en-Yveline, France). Monoclonal anti-SPARC was purchased from Haematologic Technologies Inc. (Essex Junction, VT, USA). Monoclonal MITF was purchased from Spring Bioscience (Fremont, CA, USA). Monoclonal CXCL1 and CXCR2 were purchased from R&D Systems (Lille, France).

Real-time quantitative PCR (Q-PCR)

For gene array analysis, total RNA was isolated using TRIZOL® (Invitrogen). After treatment with Dnase I, 2 μg of RNA were reverse transcribed using the High Capacity cDNA Archive random priming Kit (Applied Biosystems). The expression level of 19 genes related to melanoma secretome was evaluated using an ABI Biosystems 7900HT Sequence Detector System and the SYBR Green dye detection protocol as outlined by the manufacturer (Applied Biosystems). Gene-specific primers were designed using the Primer Express software (Applied Biosystems). Relative expression level of target genes was normalized for RNA concentrations of four different housekeeping genes (GAPDH, β-actin, HPRT and ubiquitin). For each sample, CT values for the housekeeping genes were determined for normalization purposes, and delta CT (ΔCT) between the mean of housekeeping genes values and target genes values was calculated. Relative expression level of target genes mRNA between DMSO control cells (DMSO) and ciglitazone treated cells (cigli.) was calculated using the formula ΔCTCigli.– ΔCTDMSO and expressed as fold over control (2ΔΔCT). Values represent the mean of duplicates and are representative of two independent experiments. Other Q-PCR were performed exactly as described [44].

Cell viability test

Cell viability was assessed using the *Cell Proliferation Kit II* (XTT; Roche Diagnostics, Meylan, *France*) according to the manufacturer's protocol. Cell viability is expressed as the percentage of the value in DMSO-treated cells.

ELISA

CXCL1 ELISA were performed using *Quantikine® Human CXCL1/GROα* from R&D Systems (Lille, France) according to the manufacturer's protocol.

Immunoflurescence microscopy

Monolayers prepared for fluorescent staining were grown on glass coverslips. Immunofluorescence experiments were carried out as described [12].

Western blot assays

Western blot analyses were performed as described [12].

Caspase activity

Caspase activities were carried out exactly as described [12].

Flow cytometry analysis

All flow cytometry analyses were performed using the FL2 channel of a FACScan (Becton Dickinson; Cowley, UK) and data were analyzed with CellQuest software as previously described [12]. Annexin-V staining was performed using *Annexin-V-FLUOS Staining Kit* (Roche Diagnostics, Meylan, *France*) according to the manufacturer's protocol.

Small interfering RNA

Small interfering RNAs (siRNAs) experiments were carried out exactly as described [12]. siRNA targeting CXCL1 was from Santa Cruz Biotechnology (sc-43816). siRNA targeting MITF was described previously [40]. As nonspecific control, a scramble sequence for CXCL1 or MITF siRNA was used.

Construction of the CXCL1 reporter plasmid

A 1.5-kb fragment 5' of the transcriptional site of the CXCL1 gene was amplified by PCR reaction and isolated by Topo® Cloning Kit (Invitrogen) from genomic DNA. The 1.5-kb XhoI/SacI fragment was then subcloned using Rapid DNA Ligation Kit (Roche) into the unique XhoI/SacI restriction site of the Promega pGL3 basic vector (pGL3b) upstream of the luciferase coding sequence (pCXCL1; -1477/+77).

Transfections and luciferase assays

Transfections and luciferase assays were performed as described [12]. The reporter plasmid containing the 2.2-kb fragment of the mouse tyrosinase promoter (pTyro; −2,236/+59) was described elsewhere [45]. Plasmids coding for microphthalmia coding sequence (WT Mitf) or its dominant negative form containing an inframe deletion of the NH_2-terminal domain (DN Mitf) in $pCDNA_3$ expression vector are described elsewhere [18].

Chromatin Immunoprecipitation Assay

SK-Mel-28 cells were cultured in 100-cm^2 culture dishes, stimulated or not with ciglitazone or forskolin for 24 h, and then treated with 1% formaldehyde for 10 min at room temperature. Next, the cells were harvested, centrifuged (700 X *g*, 5 min at 4 °C), and resuspended in SDS lysis buffer (EZ-ChIP™ Chromatin Immunoprecipitation Kit; Upstate). After sonication the

sheared chromatin was immunoprecipitated using indicated antibody. Then, protein/DNA cross-linking complexes were reversed by heat treatment (65°C overnight) and proteinase K digestion. The genomic captured fragments were purified using spin columns. Identification of the captured DNA fragments was performed by PCR analysis using the CXCL1 or GAPDH promoter primers. Thirty-two cycles of PCR were performed, and the amplified products were analyzed on a 2.5% agarose gel.

In vivo murine cancer model

Animal experiments were carried out in accordance with the Declaration of Helsinki and were approved by a local ethical committee. Female immune-deficient BALB/c *nu/nu* (nude) mice were obtained at 6 weeks of age from Harlan Laboratory.

Mice were inoculated subcutaneously with A375 melanoma cells ($2.5x10^6$ cells/mouse). After 19 days, animals received intraperitoneal injection of ciglitazone (50 mg/kg/day) dissolved in a mixture of Labrafil M 1944 Cs (an amphiphilic oil, Oleic Macrogol-6 Glyceride), dimethylacetamide, and Tween 80 (90:9:1%, vol/vol/vol) as previously described [46].

The growth tumor curves were determined by measuring the tumor volume using the equation $V= (LxW^2)/2$. After 11 days of treatment, mice were bled and sera were analyzed using ELISA of CXCL1. At the end of the experiment, mice were killed by CO_2 inhalation and tumors were taken for RNA extraction.

Statistical analysis

Data presented are mean +/-SD of three independent experiments performed in triplicate. Statistical significance was assessed using the Student's *t*-test except for *in vivo* experiments in which statistical significance was assessed using two-tailed Wilcoxon rank sum test. A value of $p < 0.05$ was accepted as statistically significant.

Abbreviations

BSA: Bovine Serum Albumin, DMEM: Dulbecco's Modified Eagle's Medium, DMSO: Dymethylsulfoxyde, ELISA: Enzyme Linked ImmunoSorbent Assay, FCS: Fetal Calf Serum, IBMX: 3-IsoButyl-1-MethylXanthine, NHM: Normal Human Melanocytes, PARP: Poly(ADP-Ribose) Polymerase, PPARγ: Peroxysome Proliferator activated receptor gamma, TNFα: Tumor Necrosis Factor alpha, TZD: thiazolidinedione.

Conflict of interest

The authors declare no conflict of interest.

Acknowledgements

We thank Dr Jeff Lacey for critical reading of the paper. Our research was supported by INSERM, University of Nice Sophia-Antipolis, Fondation pour la Recherche Médicale (FRM) and ARC grant (#5093). Thomas Botton is a recipient of a doctoral fellowship from the Ministère de l'Enseignement Supérieur et de la Recherche and from ARC (France).

References

1. Herlyn, M and Satyamoorthy, K, (1996) Activated ras. Yet another player in melanoma? Am J Pathol 149: 739-44.
2. Brose, MS, Volpe, P, Feldman, M, Kumar, M, Rishi, I, Gerrero, R et al., (2002) BRAF and RAS mutations in human lung cancer and melanoma. Cancer Res 62: 6997-7000.
3. Davies, H, Bignell, GR, Cox, C, Stephens, P, Edkins, S, Clegg, S et al., (2002) Mutations of the BRAF gene in human cancer. Nature 417: 949-54.
4. Villanueva, J and Herlyn, M, (2008) Melanoma and the tumor microenvironment. Curr Oncol Rep 10: 439-46.
5. Demierre, MF, (2006) Epidemiology and prevention of cutaneous melanoma. Curr Treat Options Oncol. 7: 181-6.
6. Chang, TH and Szabo, E, (2000) Induction of differentiation and apoptosis by ligands of peroxisome proliferator-activated receptor gamma in non-small cell lung cancer. Cancer Res. 60: 1129-38.
7. Grommes, C, Landreth, GE and Heneka, MT, (2004) Antineoplastic effects of peroxisome proliferator-activated receptor gamma agonists. Lancet Oncol 5: 419-29.
8. Hisatake, JI, Ikezoe, T, Carey, M, Holden, S, Tomoyasu, S and Koeffler, HP, (2000) Down-Regulation of prostate-specific antigen expression by ligands for peroxisome proliferator-activated receptor gamma in human prostate cancer. Cancer Res. 60: 5494-8.
9. Kubota, T, Koshizuka, K, Williamson, EA, Asou, H, Said, JW, Holden, S et al., (1998) Ligand for peroxisome proliferator-activated receptor gamma (troglitazone) has potent antitumor effect against human prostate cancer both in vitro and in vivo. Cancer Res. 58: 3344-52.
10. Sarraf, P, Mueller, E, Jones, D, King, FJ, DeAngelo, DJ, Partridge, JB et al., (1998) Differentiation and reversal of malignant changes in colon cancer through PPARgamma. Nat Med. 4: 1046-52.
11. Toyoda, M, Takagi, H, Horiguchi, N, Kakizaki, S, Sato, K, Takayama, H et al., (2002) A ligand for peroxisome proliferator activated receptor gamma inhibits cell growth and induces apoptosis in human liver cancer cells. Gut. 50: 563-7.
12. Botton, T, Puissant, A, Bahadoran, P, Annicotte, JS, Fajas, L, Ortonne, JP et al., (2009) In Vitro and In Vivo Anti-Melanoma Effects of Ciglitazone. J Invest Dermatol.
13. Haghnegahdar, H, Du, J, Wang, D, Strieter, RM, Burdick, MD, Nanney, LB et al., (2000) The tumorigenic and angiogenic effects of MGSA/GRO proteins in melanoma. J Leukoc Biol 67: 53-62.
14. Luan, J, Shattuck-Brandt, R, Haghnegahdar, H, Owen, JD, Strieter, R, Burdick, M et al., (1997) Mechanism and biological significance of constitutive expression of MGSA/GRO chemokines in malignant melanoma tumor progression. J Leukoc Biol 62: 588-97.
15. Bordoni, R, Fine, R, Murray, D and Richmond, A, (1990) Characterization of the role of melanoma growth stimulatory activity (MGSA) in the growth of normal melanocytes, nevocytes, and malignant melanocytes. J Cell Biochem 44: 207-19.
16. Dhawan, P and Richmond, A, (2002) Role of CXCL1 in tumorigenesis of melanoma. J Leukoc Biol 72: 9-18.
17. Hodgkinson, CA, Moore, KJ, Nakayama, A, Steingrimsson, E, Copeland, NG, Jenkins, NA et al., (1993) Mutations at the mouse microphthalmia locus are associated with defects in a gene encoding a novel basic-helix-loop-helix-zipper protein. Cell 74: 395-404.
18. Bertolotto, C, Abbe, P, Hemesath, TJ, Bille, K, Fisher, DE, Ortonne, JP et al., (1998) Microphthalmia gene product as a signal transducer in cAMP-induced differentiation of melanocytes. J Cell Biol 142: 827-35.
19. Hughes, AE, Newton, VE, Liu, XZ and Read, AP, (1994) A gene for Waardenburg syndrome type 2 maps close to the human homologue of the microphthalmia gene at chromosome 3p12-p14.1. Nat Genet 7: 509-12.
20. Steingrimsson, E, Copeland, NG and Jenkins, NA, (2004) Melanocytes and the microphthalmia transcription factor network. Annu Rev Genet 38: 365-411.

21. Garraway, LA, Widlund, HR, Rubin, MA, Getz, G, Berger, AJ, Ramaswamy, S et al., (2005) Integrative genomic analyses identify MITF as a lineage survival oncogene amplified in malignant melanoma. Nature 436: 117-22.
22. Grabacka, M, Placha, W, Urbanska, K, Laidler, P, Plonka, PM and Reiss, K, (2008) PPAR gamma regulates MITF and beta-catenin expression and promotes a differentiated phenotype in mouse melanoma S91. Pigment Cell Melanoma Res 21: 388-96.
23. Smith, AG, Beaumont, KA, Smit, DJ, Thurber, AE, Cook, AL, Boyle, GM et al., (2009) PPARgamma agonists attenuate proliferation and modulate Wnt/beta-catenin signalling in melanoma cells. Int J Biochem Cell Biol 41: 844-52.
24. Freudlsperger, C, Moll, I, Schumacher, U and Thies, A, (2006) Anti-proliferative effect of peroxisome proliferator-activated receptor gamma agonists on human malignant melanoma cells in vitro. Anticancer Drugs 17: 325-32.
25. Kang, HY, Lee, JY, Lee, JS and Choi, YM, (2006) Peroxisome proliferator-activated receptors-gamma activator, ciglitazone, inhibits human melanocyte growth through induction of apoptosis. Arch Dermatol Res. 297: 472-6. Epub 2006 Feb 11.
26. Placha, W, Gil, D, Dembinska-Kiec, A and Laidler, P, (2003) The effect of PPARgamma ligands on the proliferation and apoptosis of human melanoma cells. Melanoma Res 13: 447-56.
27. Ueda, Y and Richmond, A, (2006) NF-kappaB activation in melanoma. Pigment Cell Res 19: 112-24.
28. Richmond, A, Yang, J and Su, Y, (2009) The Good and the Bad of Chemokines/Chemokine Receptors in Melanoma. Pigment Cell Melanoma Res.
29. Zlotnik, A and Yoshie, O, (2000) Chemokines: a new classification system and their role in immunity. Immunity 12: 121-7.
30. Payne, AS and Cornelius, LA, (2002) The role of chemokines in melanoma tumor growth and metastasis. J Invest Dermatol 118: 915-22.
31. Yang, J, Luan, J, Yu, Y, Li, C, DePinho, RA, Chin, L et al., (2001) Induction of melanoma in murine macrophage inflammatory protein 2 transgenic mice heterozygous for inhibitor of kinase/alternate reading frame. Cancer Res 61: 8150-7.
32. Dong, G, Loukinova, E, Chen, Z, Gangi, L, Chanturita, TI, Liu, ET et al., (2001) Molecular profiling of transformed and metastatic murine squamous carcinoma cells by differential display and cDNA microarray reveals altered expression of multiple genes related to growth, apoptosis, angiogenesis, and the NF-kappaB signal pathway. Cancer Res 61: 4797-808.
33. Norgauer, J, Metzner, B and Schraufstatter, I, (1996) Expression and growth-promoting function of the IL-8 receptor beta in human melanoma cells. J Immunol 156: 1132-37.
34. Lawson, DH, Thomas, HG, Roy, RG, Gordon, DS, Chawla, RK, Nixon, DW et al., (1987) Preparation of a monoclonal antibody to a melanoma growth-stimulatory activity released into serum-free culture medium by Hs0294 malignant melanoma cells. J Cell Biochem 34: 169-85.
35. Caunt, M, Hu, L, Tang, T, Brooks, PC, Ibrahim, S and Karpatkin, S, (2006) Growth-regulated oncogene is pivotal in thrombin-induced angiogenesis. Cancer Res 66: 4125-32.
36. Wang, D, Wang, H, Brown, J, Daikoku, T, Ning, W, Shi, Q et al., (2006) CXCL1 induced by prostaglandin E2 promotes angiogenesis in colorectal cancer. J Exp Med 203: 941-51.
37. Kelly, D, Campbell, JI, King, TP, Grant, G, Jansson, EA, Coutts, AG et al., (2004) Commensal anaerobic gut bacteria attenuate inflammation by regulating nuclear-cytoplasmic shuttling of PPAR-gamma and RelA. Nat Immunol 5: 104-12.
38. Ricote, M, Li, AC, Willson, TM, Kelly, CJ and Glass, CK, (1998) The peroxisome proliferator-activated receptor-gamma is a negative regulator of macrophage activation. Nature 391: 79-82.
39. Wang, LH, Yang, XY, Zhang, X and Farrar, WL, (2007) Inhibition of adhesive interaction between multiple myeloma and bone marrow stromal cells by PPARgamma cross talk with NF-kappaB and C/EBP. Blood 110: 4373-84.
40. Larribere, L, Hilmi, C, Khaled, M, Gaggioli, C, Bille, K, Auberger, P et al., (2005) The cleavage of microphthalmia-associated transcription factor, MITF, by caspases plays an essential role in melanocyte and melanoma cell apoptosis. Genes Dev 19: 1980-5.

41. Gaggioli, C, Robert, G, Bertolotto, C, Bailet, O, Abbe, P, Spadafora, A et al., (2006) Tumor-Derived Fibronectin Is Involved in Melanoma Cell Invasion and Regulated by V600E B-Raf Signaling Pathway. J Invest Dermatol 7: 7.
42. Larribere, L, Khaled, M, Tartare-Deckert, S, Busca, R, Luciano, F, Bille, K et al., (2004) PI3K mediates protection against TRAIL-induced apoptosis in primary human melanocytes. Cell Death Differ 11: 1084-91.
43. Li, G, Satyamoorthy, K, Meier, F, Berking, C, Bogenrieder, T and Herlyn, M, (2003) Function and regulation of melanoma-stromal fibroblast interactions: when seeds meet soil. Oncogene. 22: 3162-71.
44. Beuret, L, Flori, E, Denoyelle, C, Bille, K, Busca, R, Picardo, M et al., (2007) Up-regulation of MET expression by alpha-melanocyte-stimulating hormone and MITF allows hepatocyte growth factor to protect melanocytes and melanoma cells from apoptosis. J Biol Chem 282: 14140-7.
45. Bertolotto, C, Bille, K, Ortonne, JP and Ballotti, R, (1996) Regulation of tyrosinase gene expression by cAMP in B16 melanoma cells involves two CATGTG motifs surrounding the TATA box: implication of the microphthalmia gene product. J Cell Biol 134: 747-55.
46. Miot-Noirault, E, Legault, J, Cachin, F, Mounetou, E, Degoul, F, Gaudreault, RC et al., (2004) Antineoplastic potency of arylchloroethylurea derivatives in murine colon carcinoma. Invest New Drugs 22: 369-78.

Figure Legends

Figure 1: Ciglitazone modifies melanoma cell secretome.

a) Starved normal human melanocytes (NHM) were treated or not with 10µM ciglitazone (Cigli.) for 96 hrs. Cells were then harvested and counted using trypan blue. Results are expressed in percent of control (100%).

b) Starved A375 melanoma cells were treated or not with 10µM ciglitazone for 24 hours. Conditioned media were collected and centrifuged for 5 minutes at 2000 rpm. Supernatants were immediately added to the culture medium of NHM (1:1). After 96 hours, NHM were harvested and counted using trypan blue. Results are expressed in percent of control (100%). Data are mean +/- SD of three independent experiments performed in triplicate. Significantly different from the corresponding control ** $p< 0.01$.

Figure 2: Ciglitazone decreases CXCL1 level in A375 melanoma cells.

Starved A375 melanoma cells were treated for 24 hours with various concentrations of ciglitazone or TNFα (10ng/ml).

a) Total RNA was extracted and analyzed by real-time quantitative PCR using *CXCL1* primers. mRNA expression was normalized using *SB34* RNA level. Results are expressed as a mean +/- SD from 3 independent experiments. Significantly different from the corresponding control * $p< 0.05$; ** $p< 0.01$; *** $p< 0.001$.

b) A375 cells were fixed and stained for CXCL1 or CXCR2 (green) and with DAPI (blue). DAPI staining was used to identify cell nucleus. Right panels show merge of DAPI and CXCL1 or CXCR2 staining. Slides were examined with a Zeiss Axiophot fluorescence microscope and pictures were taken at X200 magnification. Representative field of three different experiments are shown.

c) ELISA of CXCL1 was performed on supernatants from starved A375 melanoma cells treated as indicated. Data are mean +/- SD of three independent experiments performed in triplicate. SPARC western blotting on those supernatants was used as loading control. Significantly different from the corresponding control * $p< 0.05$; *** $p< 0.001$.

Figure 3: CXCL1 expression in response to various TZD and in different cell lines

a) Time course of XTT activity (upper panel) and ELISA assay for CXCL1 (lower panel) were performed on starved A375 melanoma cells treated for different times with 1 or 10 µM ciglitazone or with staurosporine. Results are expressed in percent of control (100%) for each time. Data are mean +/- SD of three independent experiments performed in triplicate.

b) ELISA of CXCL1 was performed on supernatants from starved A375 melanoma cells treated for 24 hours with different TZD: ciglitazone (Cigli.), pioglitazone (Pio.), rosiglitazone (Rosi.), troglitazone (Trogli.). Results are expressed in percent of control (100%) for each time. Data are mean +/- SD of three independent experiments performed in triplicate.

c) ELISA of CXCL1 was performed on supernatants from starved normal human melanocytes (NHM) treated or not for 24 hours with various concentrations of ciglitazone added or not with TNFα 10 ng/ml. Data are mean +/- SD of three independent experiments performed in triplicate.

d) ELISA of CXCL1 was performed on supernatants from different cell lines treated or not for 24 hours with 10µM of ciglitazone added or not with TNFα 10 ng/ml. Data are mean +/- SD of three independent experiments performed in triplicate. Significantly different from the corresponding control * p< 0.05; ** p< 0.01; *** p< 0.001; # p< 0.05.

e) Starved cells from various cell lines were treated or not with 10µM ciglitazone for 60 hrs. Cells were then harvested and counted using trypan blue. Results are expressed in percent of control (100%). Data are mean +/- SD of three independent experiments performed in triplicate.

Figure 4: Recombinant CXCL1 is sufficient to abrogate decrease of cell viability induced by ciglitazone.

XTT activity was performed on starved A375 melanoma cells treated with ciglitazone 10µM added or not with various concentrations of recombinant CXCL1 **(a)**, 10 ng/ml TNFα **(b)** or treated with various concentrations of TRAIL or staurosporine added with 50 ng/ml of recombinant CXCL1 **(c)**. Results are expressed in percent of control (100%) for each time. Data are mean +/- SD of three independent experiments performed in triplicate. Significantly different from the corresponding control * p< 0.05; *** p< 0.001.

Figure 5: Recombinant CXCL1 is sufficient to abrogate apoptosis induced by ciglitazone.

Starved A375 melanoma cells were treated for 24 hours with various concentrations of ciglitazone added or not with 50 ng/ml of recombinant CXCL1 (rCXCL1).

a) Western blot was performed on cell lysates (30 µg total protein per lane). Proteins were separated by 10% SDS-PAGE and analyzed by western blot using the indicated antibody. HSP60 was used as loading control. One representative experiment of three is shown.

b) Caspase 3, 8 and 9 activities were performed on cell lysates (30µg per condition). Lysate from cells treated for 5 hours with 1 µM staurosporine was used as positive control of caspases activation. Results are expressed in relative fluorescence units per minute and per mg of protein (UAF/min/mg of prot.). Data are mean +/- SD of three independent experiments performed in triplicate. Significantly different from the corresponding control; ** p< 0.01; *** p< 0.001; # p< 0.05.

c) Cells were detached and stained with Annexin-V-Fluorescein before being analyzed by flow cytometry. Data are representative of three independent experiments performed in triplicate.

Figure 6: Inhibition of CXCL1 decreases cell viability.

a) Starved A375 cells were transfected for 48 hours with various concentrations of siRNA targeting CXCL1 (si-CXCL1) or a scramble sequence (si-CT). ELISA for CXCL1 was performed on supernatants from transfected cells. Results are expressed in percent of control (100%). Data are mean +/- SD of three independent experiments performed in triplicate. SPARC western blotting on those supernatants was used as loading control. Significantly different from the corresponding control *** p< 0.001.

b) XTT activity was performed on starved A375 transfected for 48 hours with various concentrations of siRNA targeting CXCL1 and added or not with rCXCL1 (50 ng/ml).

Results are expressed in percent of cells transfected with the control siRNA (100%) for each concentration. Data are mean +/- SD of three independent experiments performed in triplicate. Significantly different from the corresponding control * $p< 0.05$; *** $p< 0.001$.

c) XTT activity was performed on starved A375 treated for 24 hours with various concentrations of blocking antibody targeting CXCL1. Results are expressed in percent of control (100%). Data are mean +/- SD of three independent experiments performed in triplicate. Significantly different from the corresponding control * $p< 0.05$; *** $p< 0.001$.

d) Caspase 3, 8 and 9 activities were performed on cell lysates (30µg per condition) from starved A375 transfected for 48 hours with various concentrations of control (CT) or CXCL1 siRNA. Results are expressed in relative fluorescence units per minute and per mg of protein (UAF/min/mg of prot.). Data are mean +/- SD of three independent experiments performed in triplicate. Significantly different from the corresponding control *** $p< 0.001$.

e) Starved A375 cells were transfected for 48 hours with 50nM of siRNA targeting CXCL1 (si-CXCL1) or a scramble sequence (si-CT). Cells were detached and stained with Annexin-V-Fluorescein before being analyzed by flow cytometry. Data are representative of three independent experiments performed in triplicate.

Figure 7: Decrease of CXCL1 mediated by ciglitazone involves MITF transcription factor.

a) On left panel, starved A375 or SK-Mel-28 melanoma cells were treated or not with 10µM ciglitazone (Cigli.) at different times. On right panel, starved SK-Mel-28 were treated for 24 hours with DMSO or ciglitazone added or not with 100µM Z-VAD-FMK.
Proteins were separated by 12% SDS-PAGE and analyzed by western blot using the indicated antibody. HSP60 was used as loading control. One representative experiment of three is shown.

b) Total RNA from starved A375 cells treated for 24 hours with various concentrations of ciglitazone was extracted and analyzed by real-time quantitative PCR using *MITF* primers. mRNA expression was normalized using *SB34* RNA levels. Results are expressed as a mean +/- SD from 3 independent experiments. Significantly different from the corresponding control * $p< 0.05$; *** $p< 0.001$.

c) Total RNA from starved A375 cells transfected for 48 hours with siRNA targeting MITF (si-MITF) or its scramble sequence (si-CT) was extracted and analyzed by real-time quantitative PCR using *MITF* and *CXCL1* primers. mRNA expression was normalized using *SB34* RNA level. Results are expressed as a mean +/- SD from 3 independent experiments. Significantly different from the corresponding control *** $p< 0.001$.

d) A375 cells transfected with the wild type form of MITF were fixed and stained for MITF (green), CXCL1 (red) and with DAPI (blue). DAPI staining was used to identify cell nucleus. Slides were examined with a Zeiss Axiophot fluorescence microscope and pictures were taken at X200 magnification. Representative field of three different experiments are shown.

e) Starved A375 melanoma cells were treated or not with 20µM forskolin (Fsk) added or not with 100µM IBMX for 7 hours. ELISA of CXCL1 was performed on supernatants from

starved A375 melanoma cells treated as described. Results are expressed in percent of control (100%). Corresponding proteins were separated by 12% SDS-PAGE and analyzed by western blot using the indicated antibody. HSP60 was used as loading control. One representative experiment of three is shown. Significantly different from the corresponding control *** p< 0.001.

f) A375 cells were transfected with vector encoding the basal luciferase construct (Mock), wild type MITF (WT MITF) or its dominant negative form (DN MITF) and with pTyro or pCXCL1 luciferase reporters. Measurement of luciferase activity was carried out 36 hours after transfection. Variability of transfection was normalized with βGal activity and results were expressed in percent of control (100%). Data are mean +/- SD of three independent experiments performed in triplicate. Significantly different from the corresponding control ** p<0.01; *** p< 0.001.

g) Chromatin immunoprecipitation assays were performed on extracts of cells treated for 24 hours with DMSO, 10µM ciglitazone (Cigli.), or with 20µM forskolin (Fsk) for 7 hours. Immunoprecipitations were performed using specific anti-MITF or anti-polymerase II (*Pol II*) antibody, and rabbit IgG (IgG) as control. Primers spanning the *CXCL1* promoter region were used for the PCR amplification. A control of PCR amplification was performed on non-immunoprecipitated extracts (*Input*). Another control was performed using a primer pair to the human GAPDH promoter.

Figure 8: ***In vivo*** **antineoplastic effects of ciglitazone correlate with decrease of MITF and CXCL1 expression.**

a) Mice were inoculated subcutaneously with A375 melanoma cells (2.5 x 10^6), and after 19 days animals (n=6 in each group) were treated with ciglitazone (50 mg/kg/day) or labrafil for 11 days. Growth tumor curves were determined by measuring the tumor volume using the equation V= (LxW^2)/2. Significantly different from the corresponding control * p< 0.05; ** p< 0.01.

b) Total RNA was extracted from mice tumors and analyzed by real-time quantitative PCR using *CXCL1* primers. mRNA expression was normalized using *SB34* RNA level. Significantly different from the corresponding control *** p< 0.001.

c) ELISA for CXCL1 was performed on mice sera from bleeding after 11 days of ciglitazone or labrafil treatment. Sera from non tumor-bearing animals were used as negative control. Data are mean +/- SD of 6 samples collected in each group. Significantly different from the corresponding control * p< 0.05. Ratio serum CXCL1/tumor volume (right panel).

d) Mice were inoculated subcutaneously with A375 melanoma cells (2.5 x 10^6), and after 12 days animals (n=6 in each group) received intraperitoneal injection of ciglitazone (50 mg/kg/day) or labrafil and subcutaneous peritumoral injections of human recombinant CXCL1 (200 ng/tumor/day) or water for 14 days. Growth tumor curves were determined by measuring the tumor volume using the equation V= (LxW^2)/2. Significantly different from Labrafil/H2O * p< 0.05; ** p< 0.01. Significant difference between Ciglitazone/H2O and Ciglitazone/CXCL1 # p< 0.05; ## p< 0.01.

Table 1: Genes differentially expressed in melanoma cells stimulated or not with ciglitazone.

The expression level of 19 genes from proteins secreted by melanomas was evaluated by real-time quantitative PCR analysis. Total RNA was extracted from A375 cells stimulated or not

with ciglitazone for 24 hours and then subjected to real-time quantitative PCR analysis as described in methods. Data are expressed in arbitrary units as fold change between DMSO-treated control cells and ciglitatone-treated cells and are a mean of two independent amplifications performed in duplicate.

A.

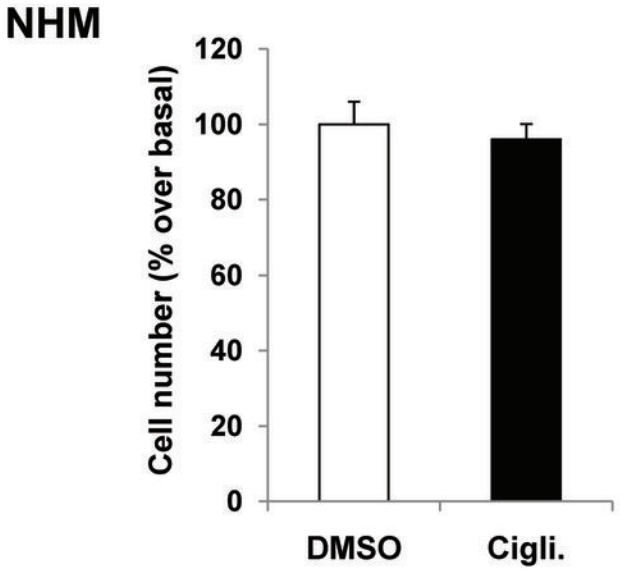

B.

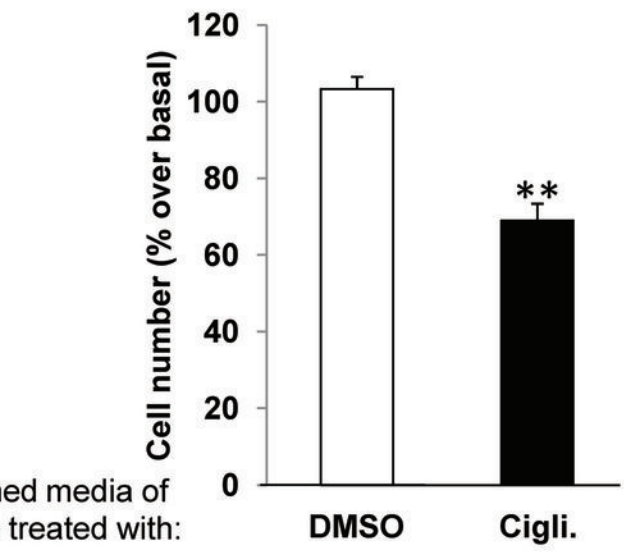

Conditioned media of A375 cells treated with:

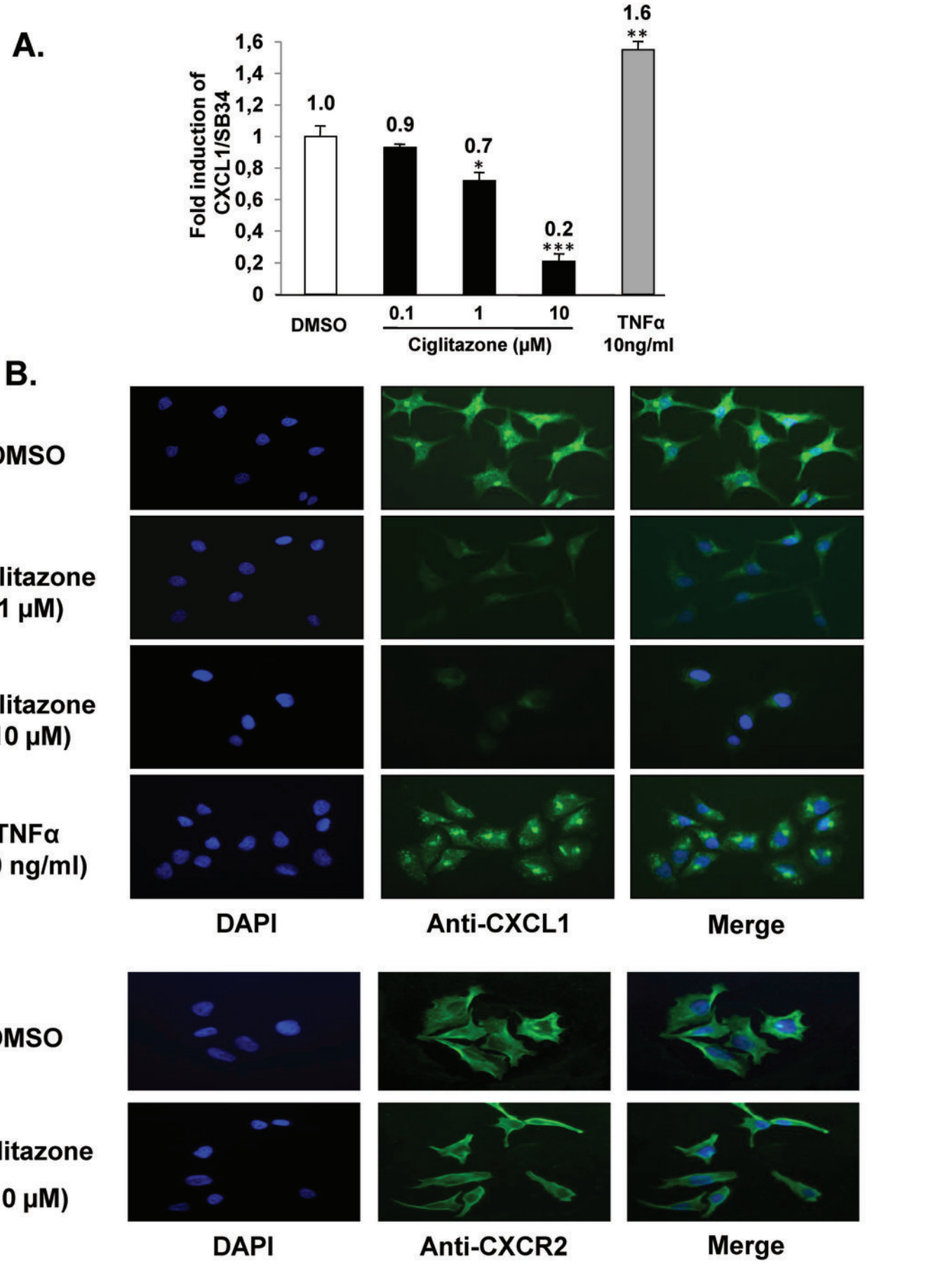
A.
Fold induction of CXCL1/SB34
1,6
1,4
1,2
1
0,8
0,6
0,4
0,2
0
1.0
0.9
0.7
*
0.2
***
1.6
**
DMSO
0.1
1
10
Ciglitazone (μM)
TNFα 10ng/ml
B.
DMSO
Ciglitazone (1 μM)
Ciglitazone (10 μM)
TNFα (10 ng/ml)
DAPI
Anti-CXCL1
Merge
DMSO
Ciglitazone (10 μM)
DAPI
Anti-CXCR2
Merge

C.

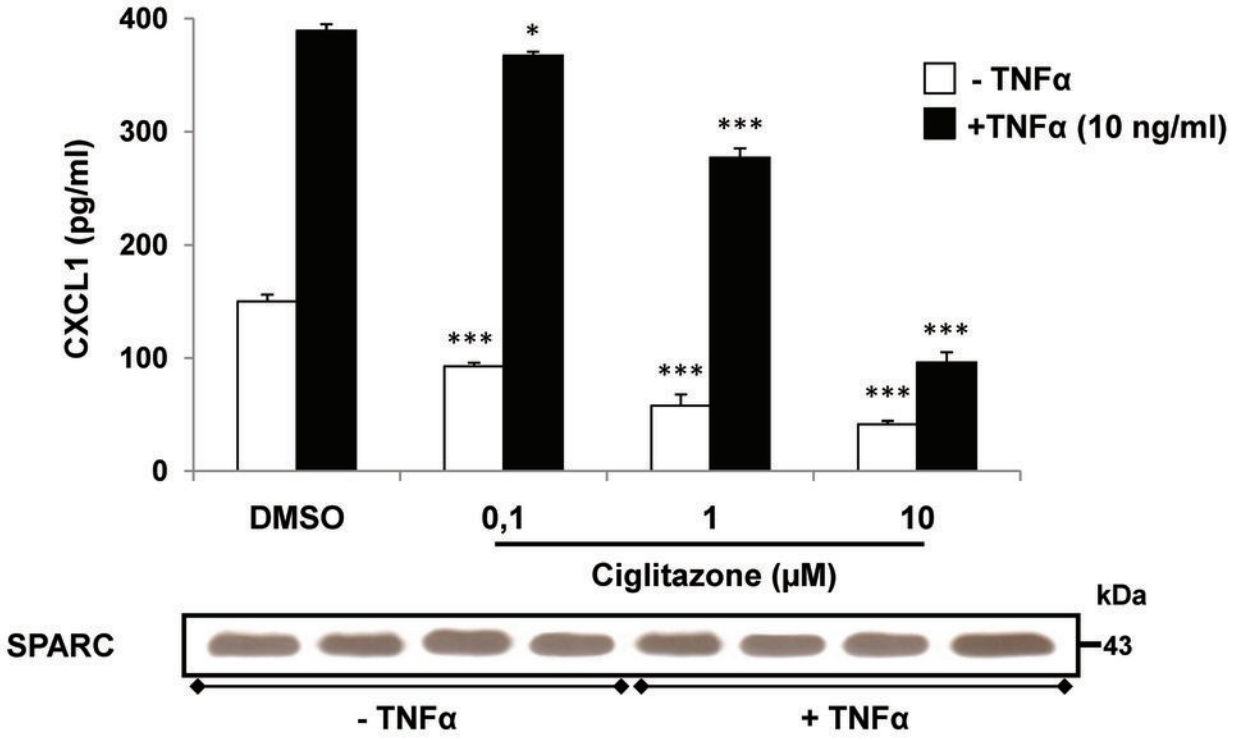
400
300
200
100
0
CXCL1 (pg/ml)
- TNFα
+TNFα (10 ng/ml)
*
***
***
***
***
DMSO
0,1
1
10
Ciglitazone (μM)
kDa
SPARC
43
- TNFα
+ TNFα

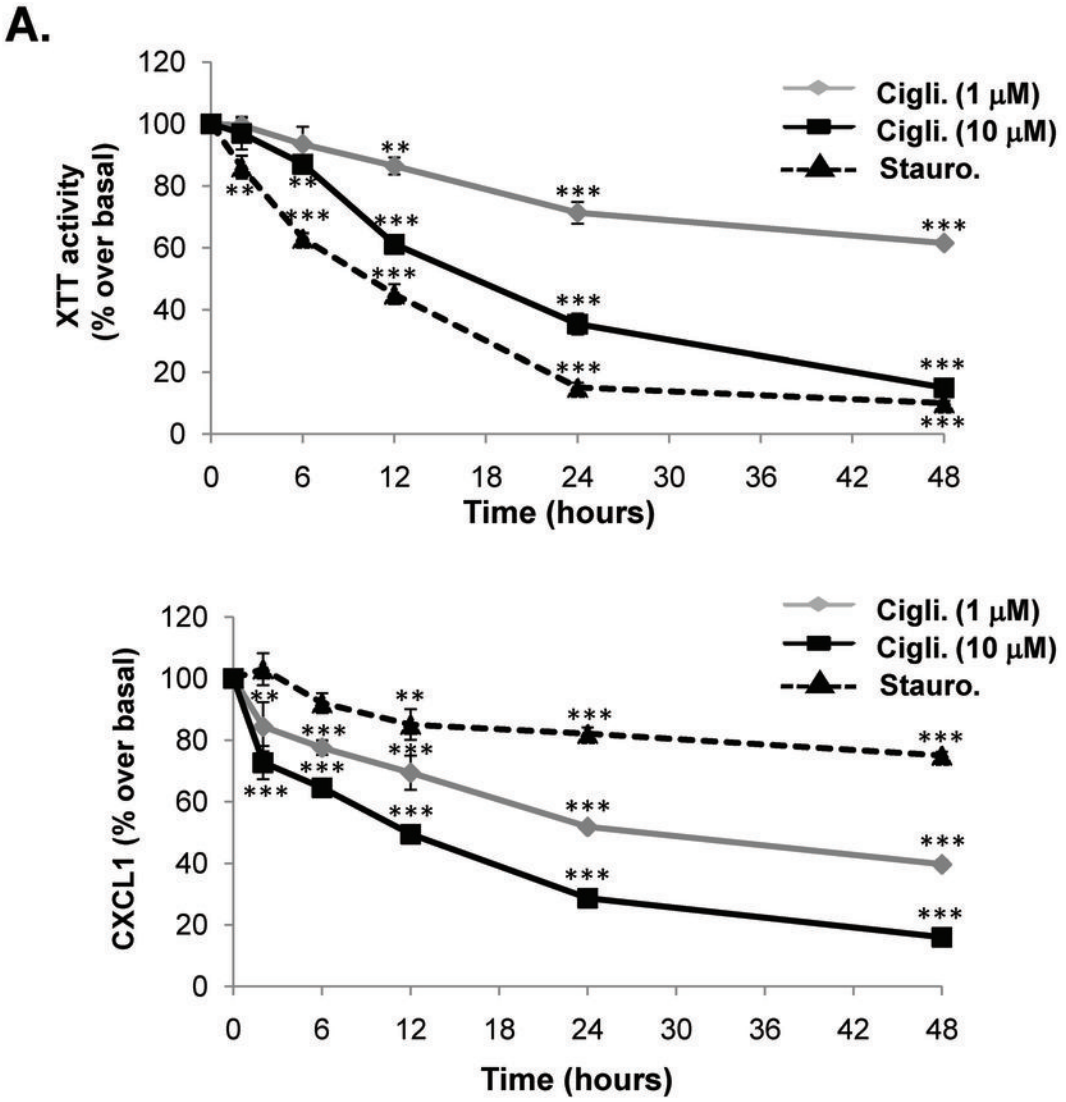
A.
XTT activity (% over basal)
Cigli. (1 μM)
Cigli. (10 μM)
Stauro.
Time (hours)
CXCL1 (% over basal)
Cigli. (1 μM)
Cigli. (10 μM)
Stauro.
Time (hours)

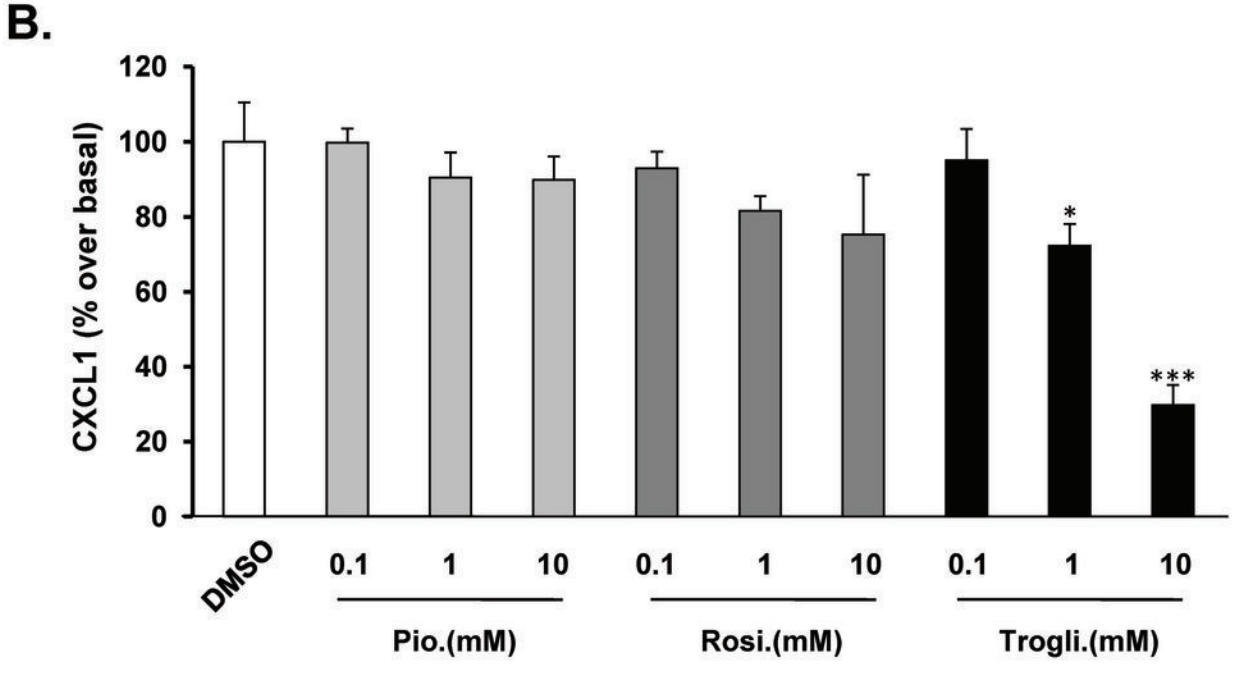
B.
CXCL1 (% over basal)
DMSO
0.1
1
10
Pio.(mM)
Rosi.(mM)
Trogli.(mM)

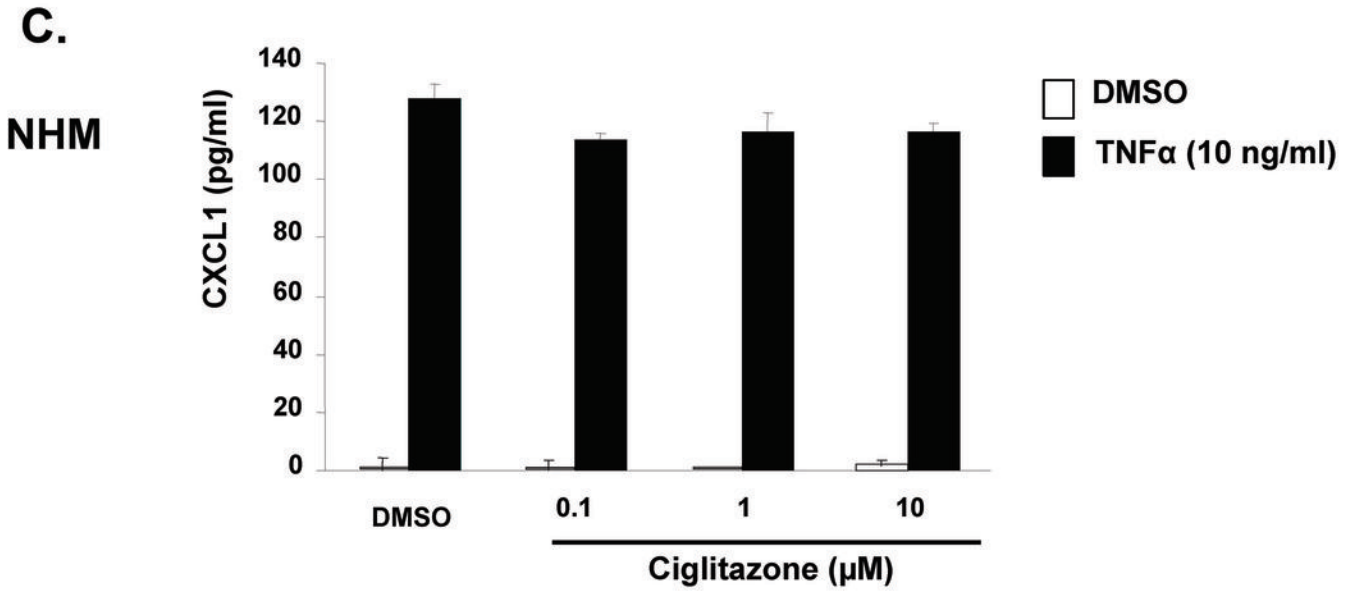
C.
NHM
CXCL1 (pg/ml)
140
120
100
80
60
40
20
0
DMSO
0.1
1
10
Ciglitazone (μM)
DMSO
TNFα (10 ng/ml)

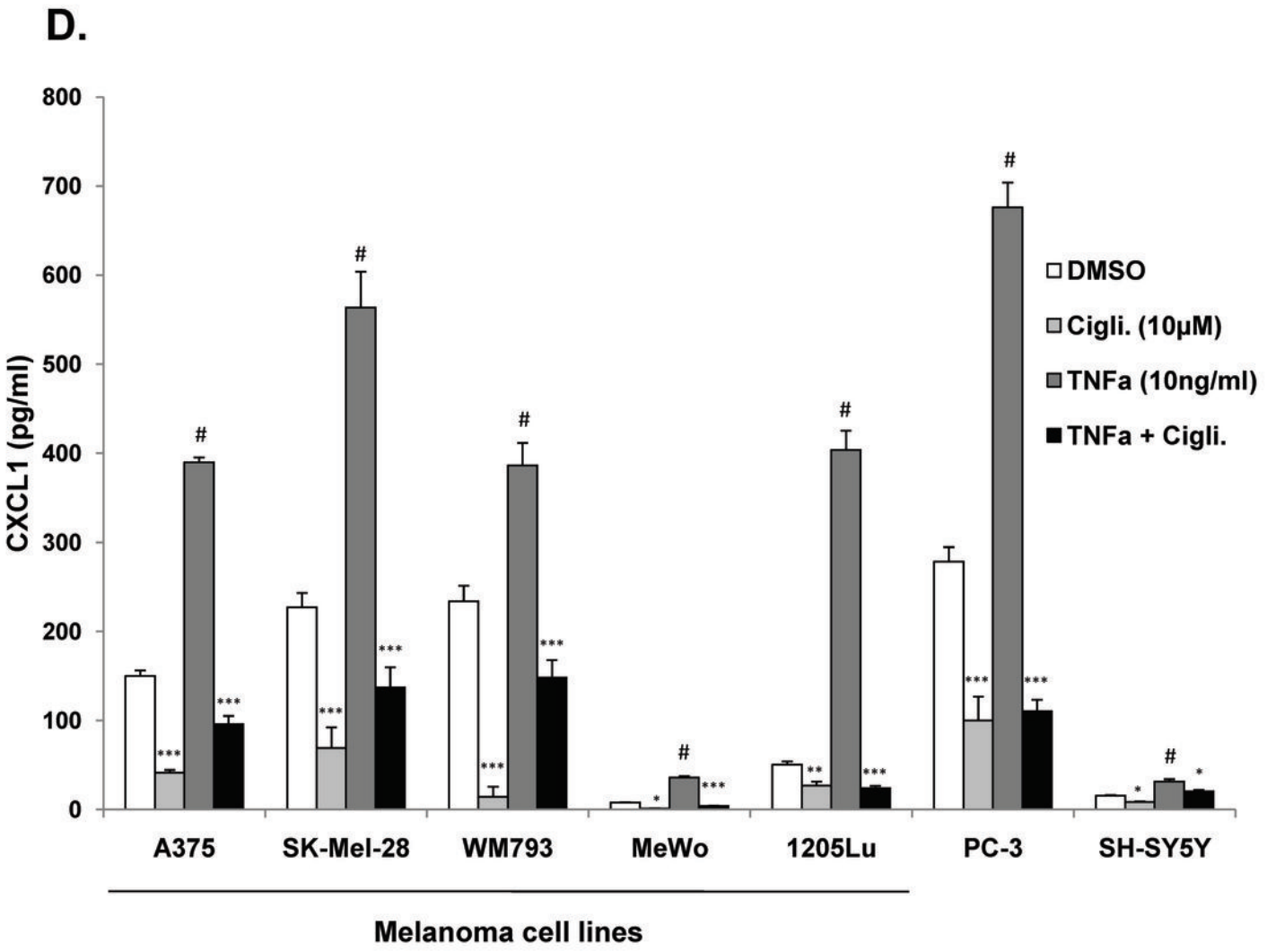
D.
CXCL1 (pg/ml)
800
700
600
500
400
300
200
100
0
DMSO
Cigli. (10μM)
TNFa (10ng/ml)
TNFa + Cigli.
A375
SK-Mel-28
WM793
MeWo
1205Lu
PC-3
SH-SY5Y
Melanoma cell lines

E.

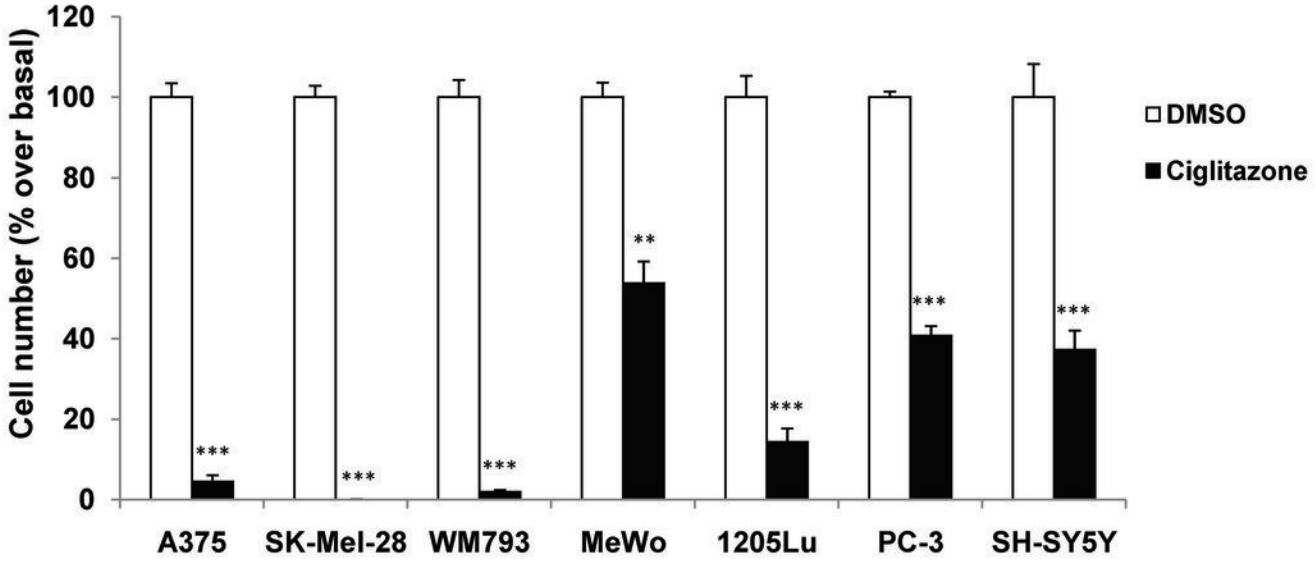
Cell number (% over basal)
120
100
80
60
40
20
0
***
***
***
**
***
***
A375
SK-Mel-28
WM793
MeWo
1205Lu
PC-3
SH-SY5Y
DMSO
Ciglitazone

Botton *et al.*, Figure 4

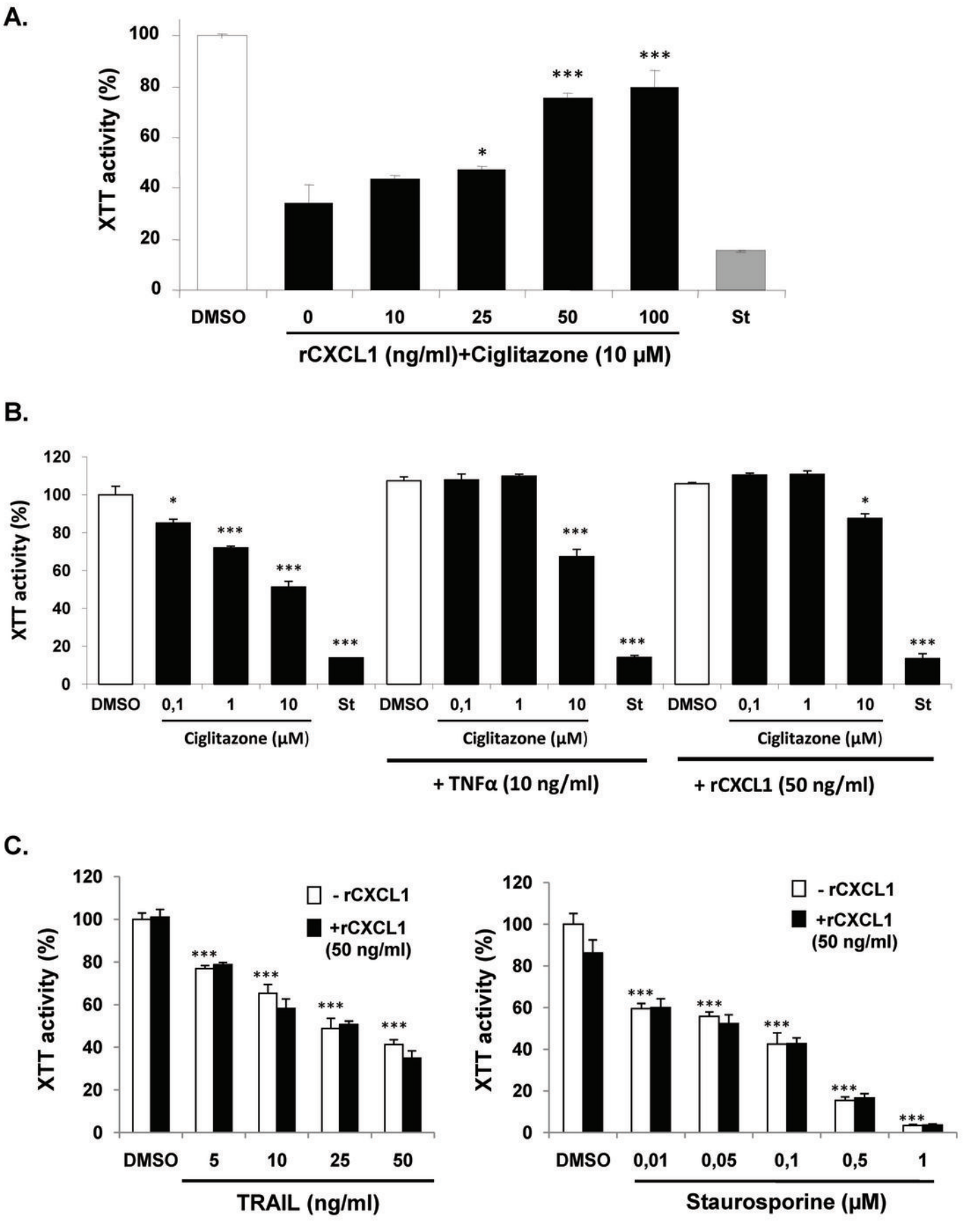

A.

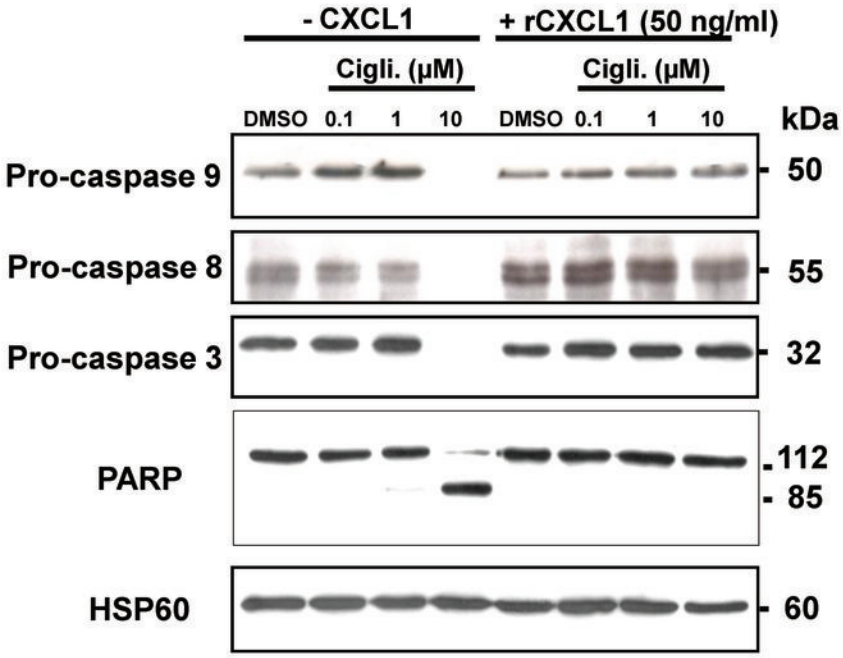
- CXCL1
+ rCXCL1 (50 ng/ml)
Cigli. (µM)
Cigli. (µM)
DMSO 0.1 1 10 DMSO 0.1 1 10
kDa
Pro-caspase 9
50
Pro-caspase 8
55
Pro-caspase 3
32
PARP
112
85
HSP60
60

B.

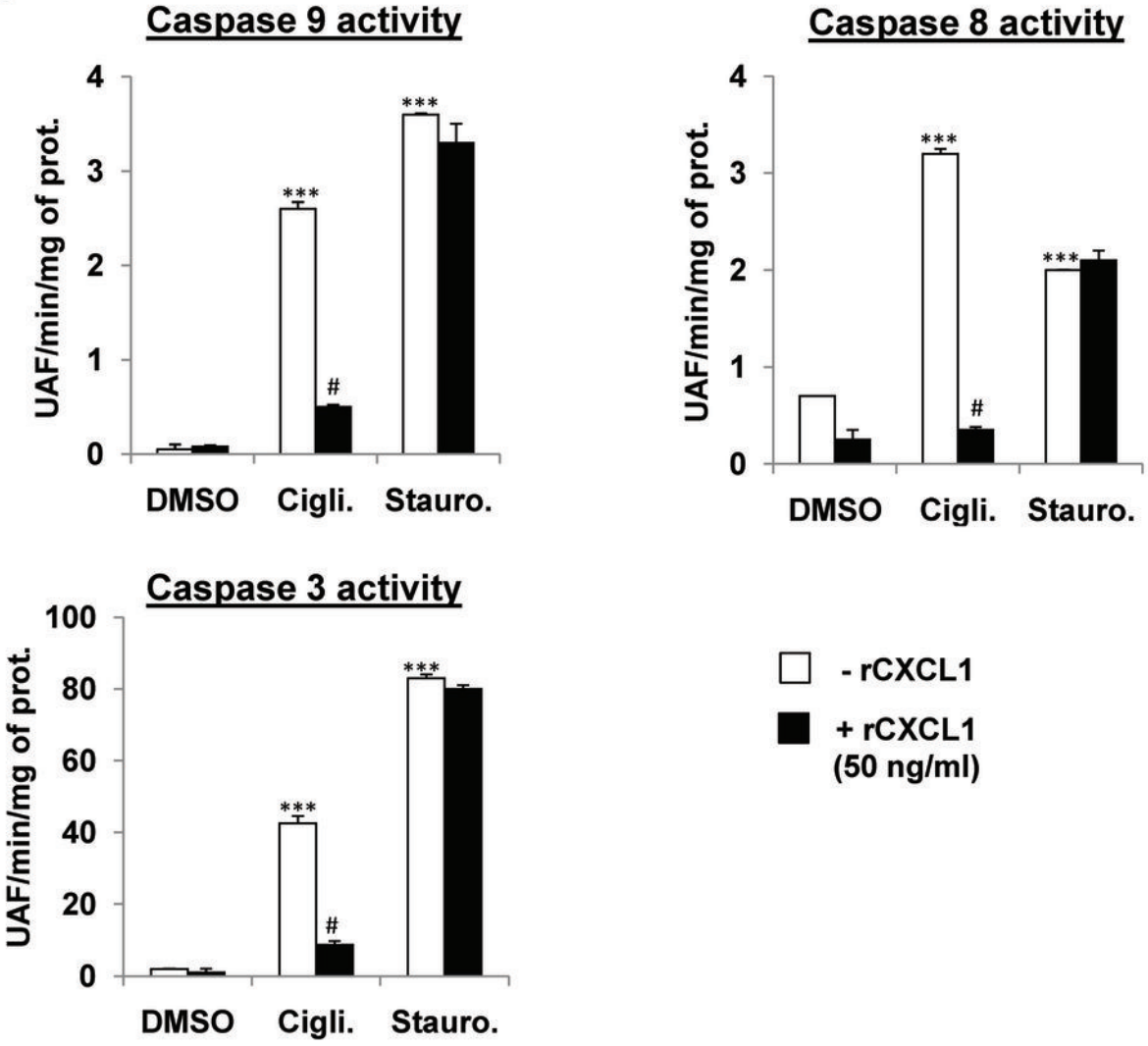
Caspase 9 activity
UAF/min/mg of prot.
DMSO
Cigli.
Stauro.
Caspase 8 activity
UAF/min/mg of prot.
DMSO
Cigli.
Stauro.
Caspase 3 activity
UAF/min/mg of prot.
DMSO
Cigli.
Stauro.
- rCXCL1
+ rCXCL1
(50 ng/ml)

C.

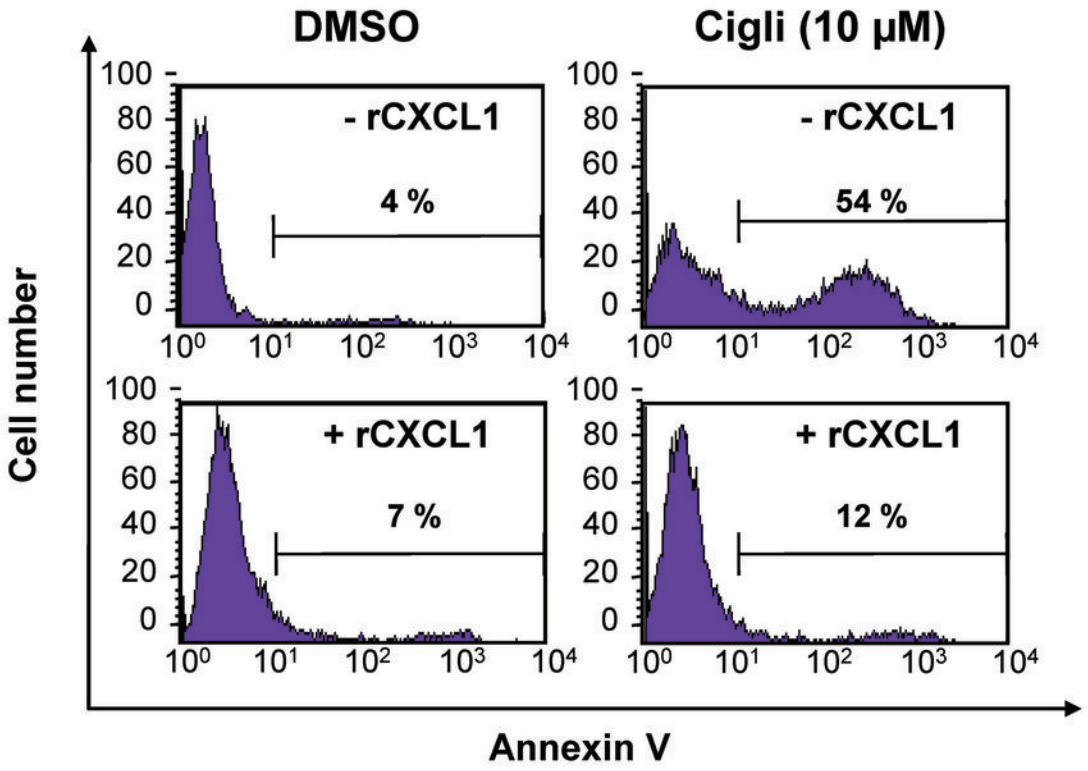
DMSO
Cigli (10 µM)
- rCXCL1
4 %
- rCXCL1
54 %
+ rCXCL1
7 %
+ rCXCL1
12 %
Cell number
Annexin V
100
80
60
40
20
0
10^0
10^1
10^2
10^3
10^4

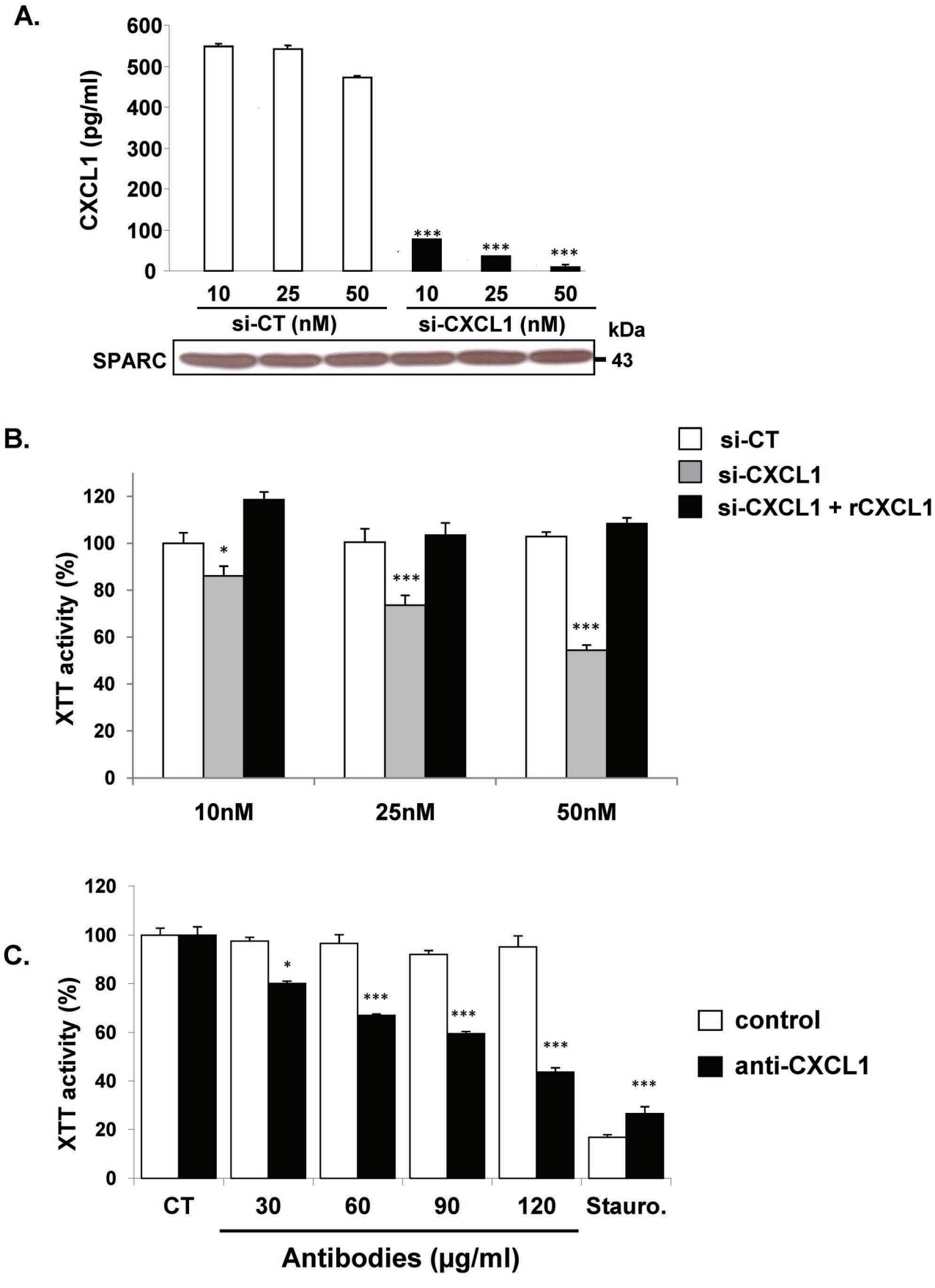
A.
CXCL1 (pg/ml)
600
500
400
300
200
100
0
***
***
***
10
25
50
10
25
50
si-CT (nM)
si-CXCL1 (nM)
kDa
SPARC
43
B.
si-CT
si-CXCL1
si-CXCL1 + rCXCL1
XTT activity (%)
120
100
80
60
40
20
0
*
***
***
10nM
25nM
50nM
C.
XTT activity (%)
120
100
80
60
40
20
0
*
***
***
***
***
control
anti-CXCL1
CT
30
60
90
120
Stauro.
Antibodies (µg/ml)

D.

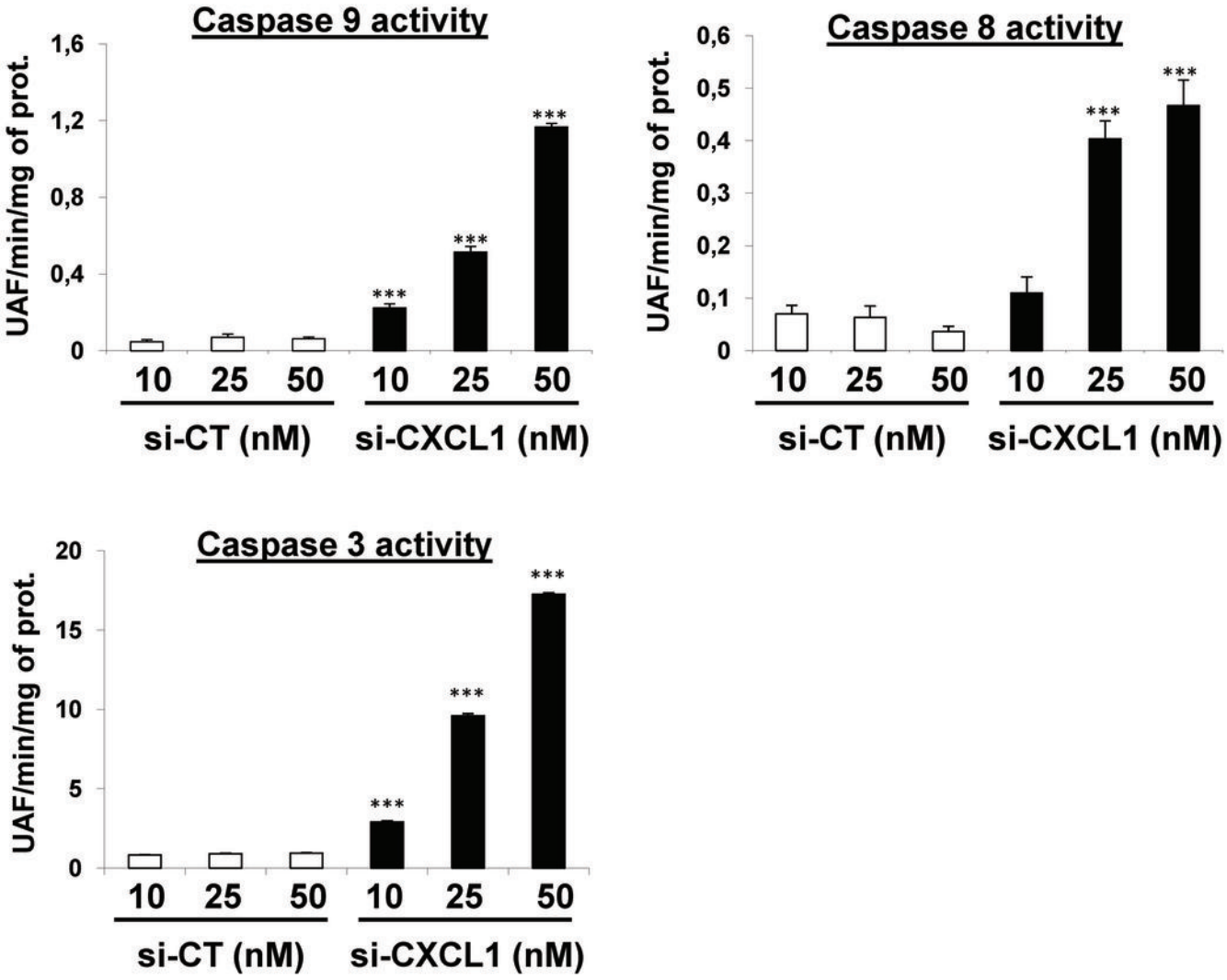
Caspase 9 activity
UAF/min/mg of prot.
1,6
1,2
0,8
0,4
0
***
10 25 50 10 25 50
si-CT (nM)
si-CXCL1 (nM)
Caspase 8 activity
UAF/min/mg of prot.
0,6
0,5
0,4
0,3
0,2
0,1
0
***
10 25 50 10 25 50
si-CT (nM)
si-CXCL1 (nM)
Caspase 3 activity
UAF/min/mg of prot.
20
15
10
5
0
***
10 25 50 10 25 50
si-CT (nM)
si-CXCL1 (nM)

E.

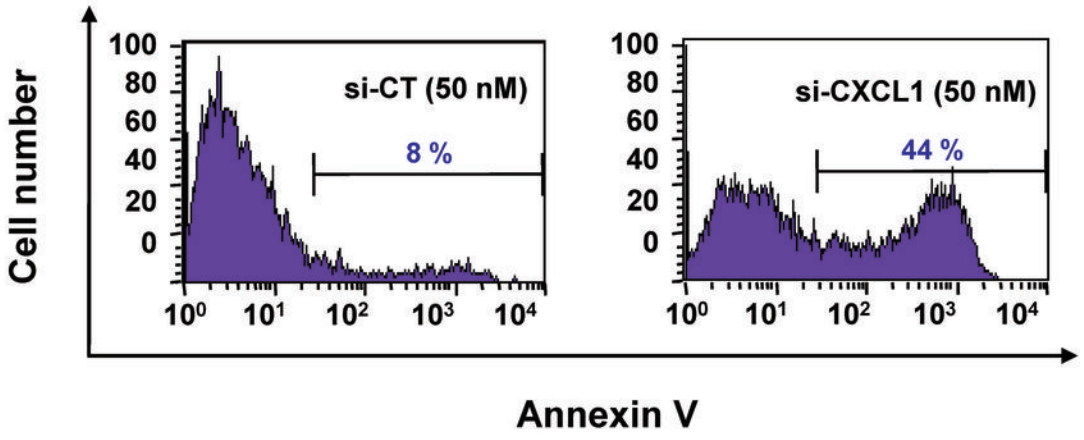
Cell number
100
80
60
40
20
0
si-CT (50 nM)
8 %
si-CXCL1 (50 nM)
44 %
10⁰ 10¹ 10² 10³ 10⁴
Annexin V

Botton *et al.*, Figure 7

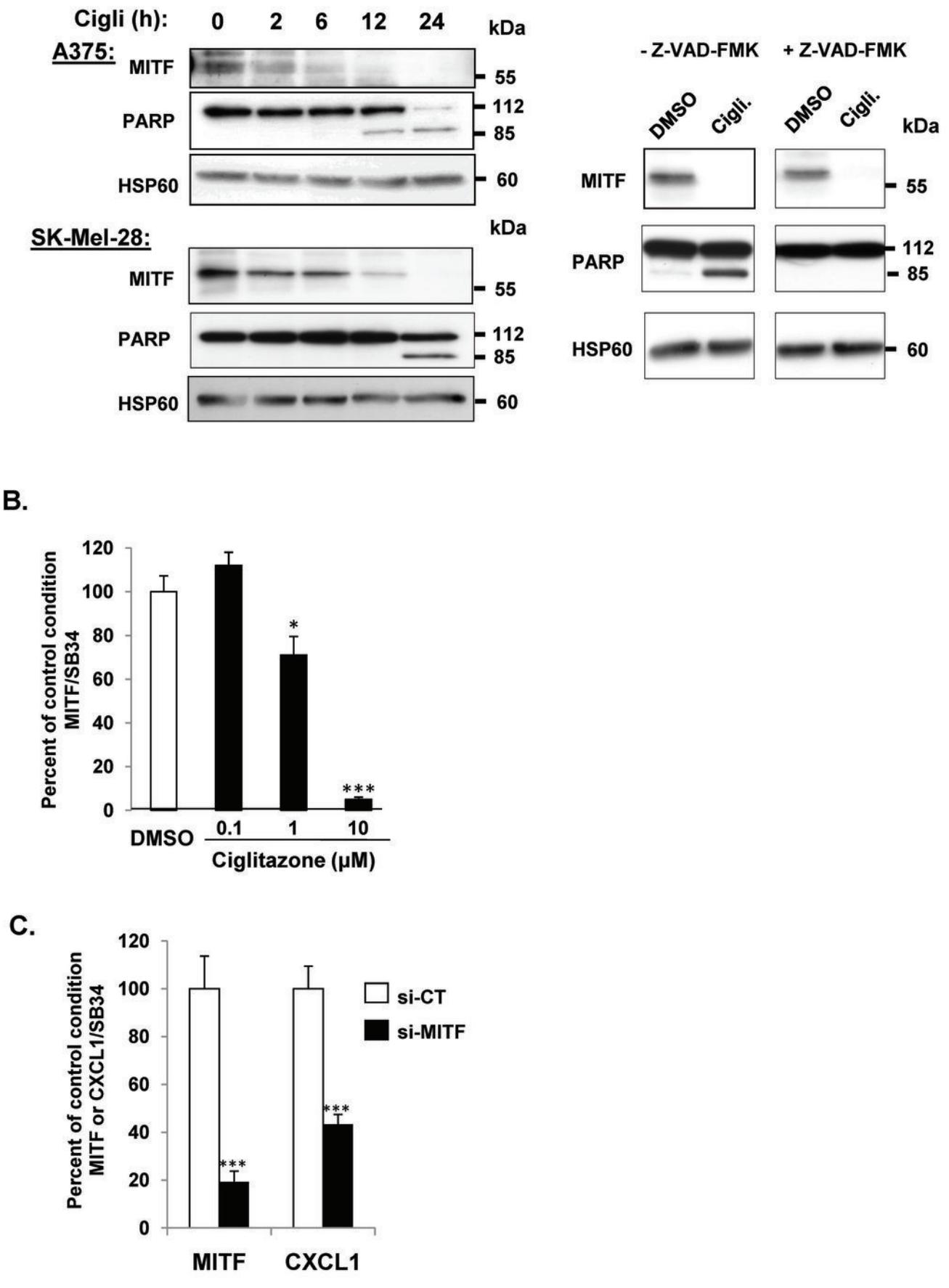

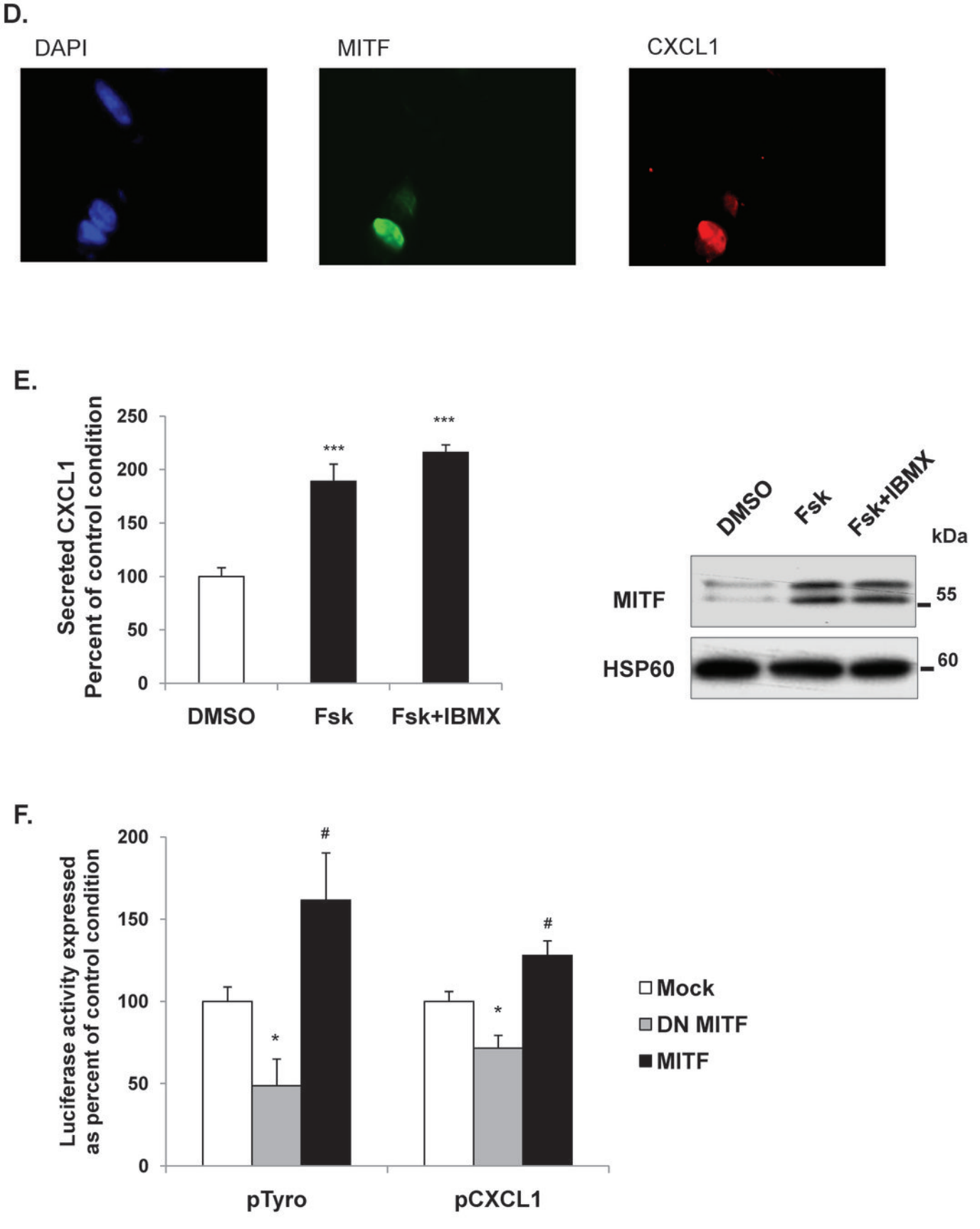
D.
DAPI
MITF
CXCL1
E.
Secreted CXCL1
Percent of control condition
250
200
150
100
50
0
***
***
DMSO
Fsk
Fsk+IBMX
DMSO
Fsk
Fsk+IBMX
kDa
MITF
55
HSP60
60
F.
Luciferase activity expressed
as percent of control condition
200
150
100
50
0
#
*
#
*
pTyro
pCXCL1
Mock
DN MITF
MITF

Botton *et al.*, Figure 7

G.

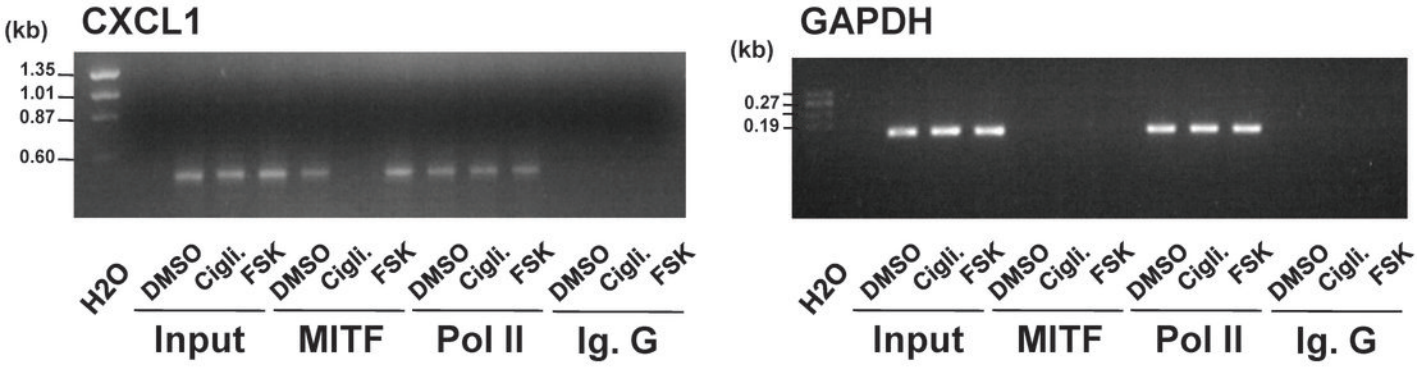

Botton *et al.*, Figure 8

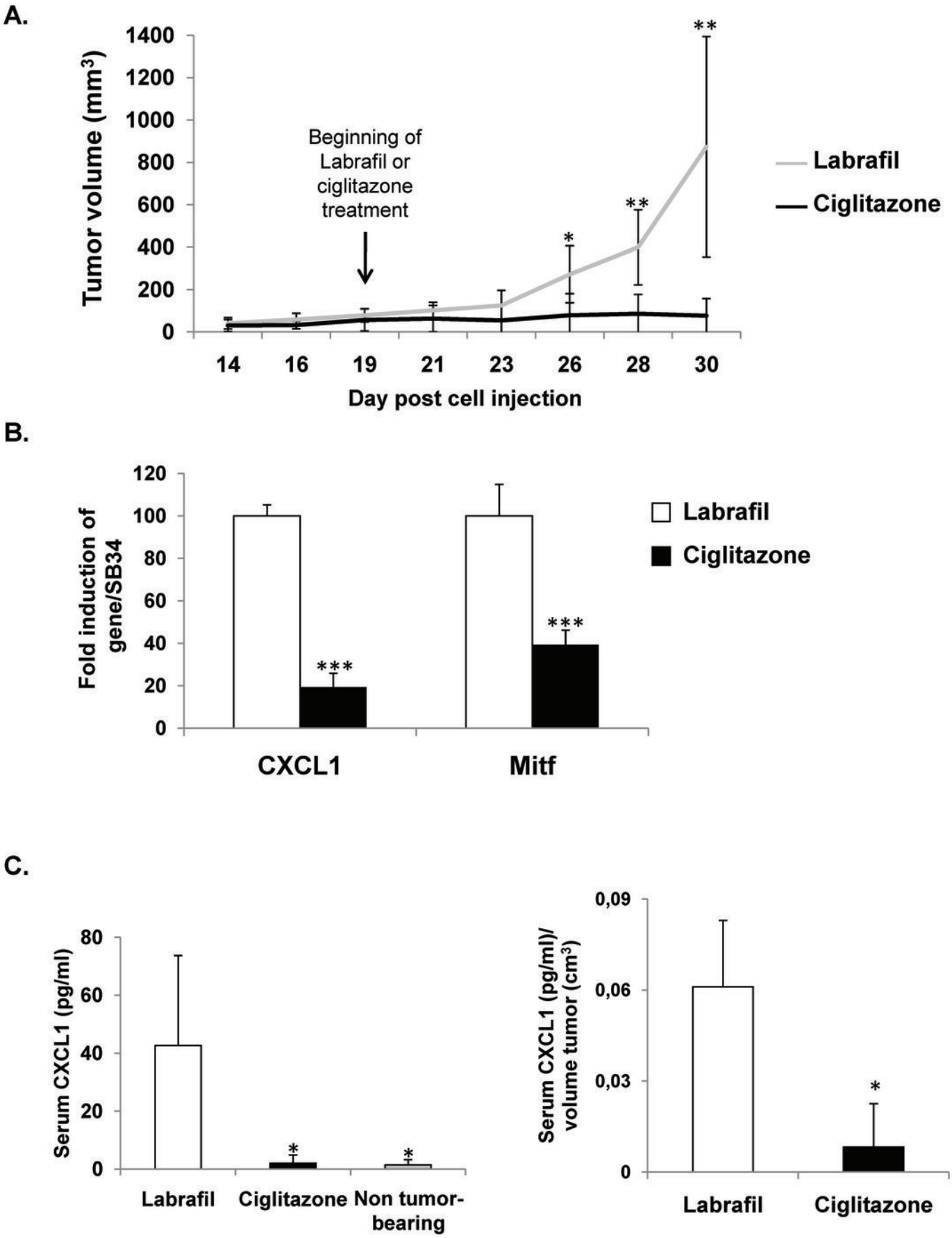

D.

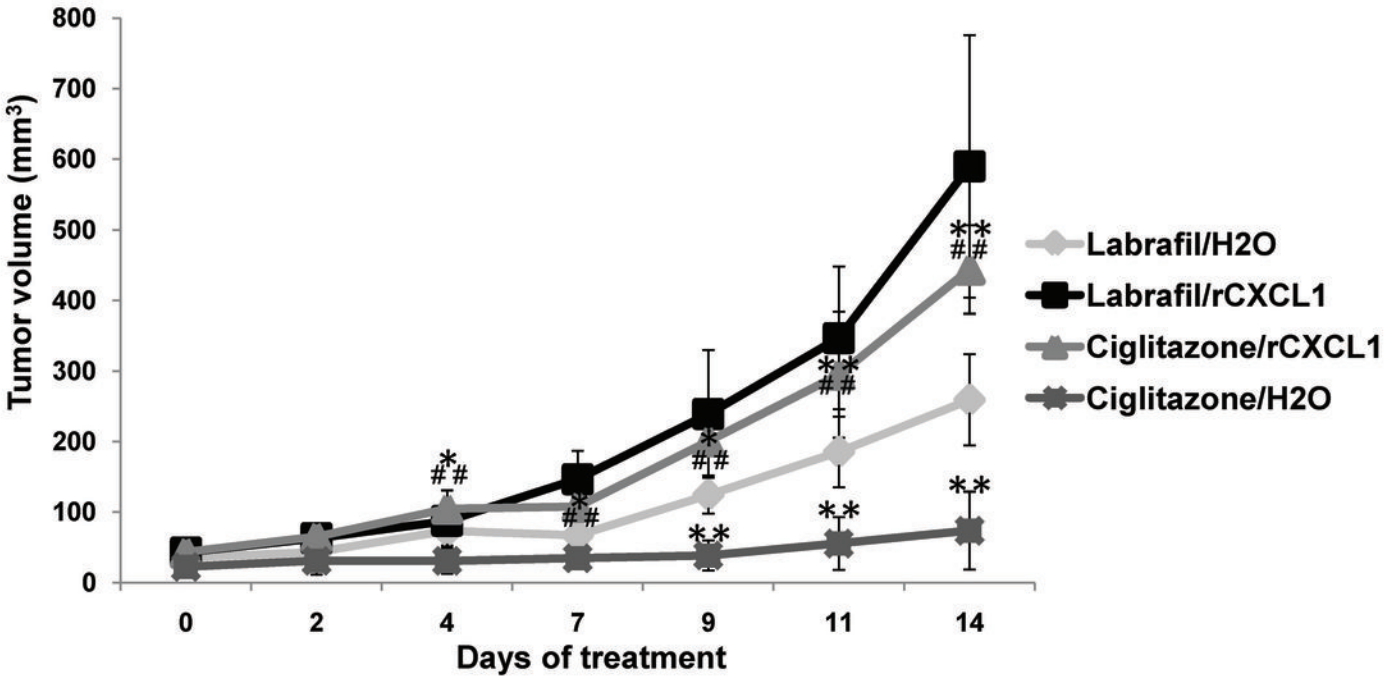
800
700
600
500
400
300
200
100
0
Tumor volume (mm3)
0
2
4
7
9
11
14
Days of treatment
Labrafil/H2O
Labrafil/rCXCL1
Ciglitazone/rCXCL1
Ciglitazone/H2O

Botton *et al.*, Table 1

Gene name	Symbol	Gene Bank ID	Fold change
Growth factors			
Epidermal growth factor	EGF	NM_001963	nd
Transforming growth factor, beta 2	TGFB2	NM_001135599	0.8
Vascular endothelial growth factor A	VEGFA	NM_001025366	0.9
Platelet-derived growth factor alpha	PDGFA	NM_002607	1.0
Hepatocyte growth factor	HGF	NM_000601	nd
Insulin-like growth factor 1	IGF1	NM_001111283	nd
Colony stimulating factor 2 (granulocyte-macrophage)	CSF2	NM_000758	1.0
Cytokines			
Chemokine (C-X-C motif) ligand 1 (melanoma growth stimulating activity, alpha)	CXCL1	NM_001511	0.4
Chemokine (C-X-C motif) ligand 2/3	CXCL2/CXCL3	NM_002089/90	0.8
Chemokine (C-X-C motif) ligand 5	CXCL5	NM_002994	1.4
Chemokine (C-C motif) ligand 2	CCL2	NM_002982	1.0
Interleukin 1, beta	IL1B	NM_000576	1.1
Interleukin 6	IL6	NM_000600	1.0
Interleukin 8	IL8	NM_000584	0.8
Others melanoma secreted proteins			
Insulin-like growth factor binding protein 7	IGFBP7	NM_001553	0.9
Endothelin 1	EDN1	NM_001955	0.9
Endothelin 2	EDN2	NM_001956	nd
Endothelin 3	EDN3	NM_000114	0.9
Wingless-type MMTV integration site family, member 3A	WNT3A	NM_033131	1.0

A.

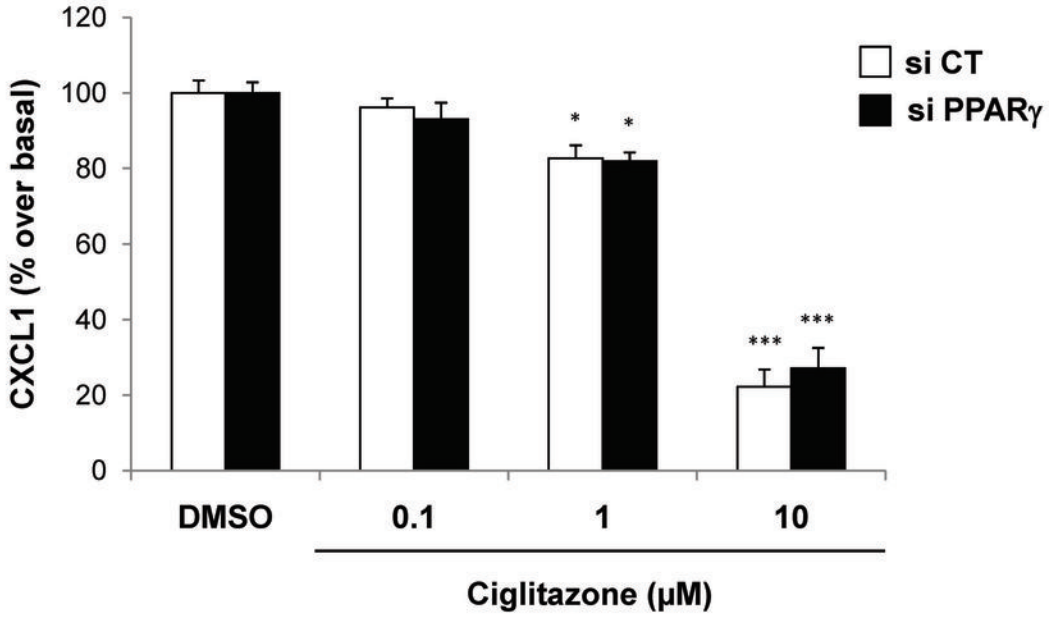
120
100
80
60
40
20
0
CXCL1 (% over basal)
si CT
si PPARγ
*
*
***
***
DMSO
0.1
1
10
Ciglitazone (μM)

B.

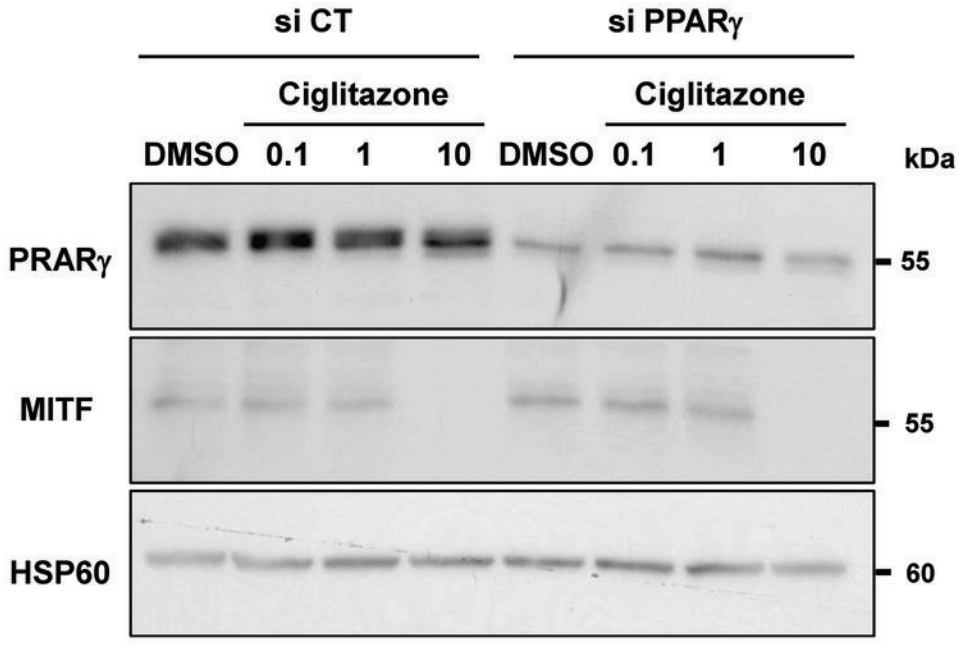
si CT
si PPARγ
Ciglitazone
Ciglitazone
DMSO
0.1
1
10
DMSO
0.1
1
10
kDa
PRARγ
55
MITF
55
HSP60
60

Botton *et al.*, Supplementary Figure S2

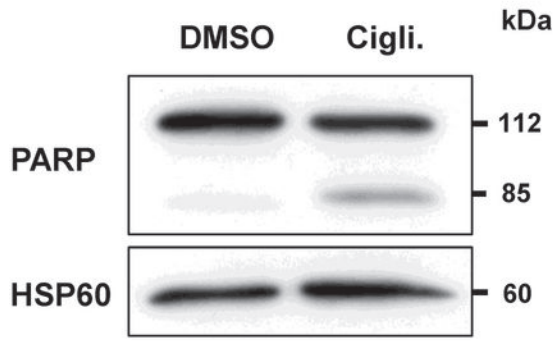

A.

	- rCXCL1				+ rCXCL1 (50 ng/ml)			
Phase (%)	DMSO	Cigli 0.1 µM	Cigli 1 µM	Cigli 10 µM	DMSO	Cigli 0.1 µM	Cigli 1 µM	Cigli 10 µM
GO/G1	69	80	80	45	66	70	71	71
S	24	11	12	7	24	20	21	20
G2/M	6	7	7	7	8	8	7	8
Sub G1	1	2	1	41	2	2	1	1

B.

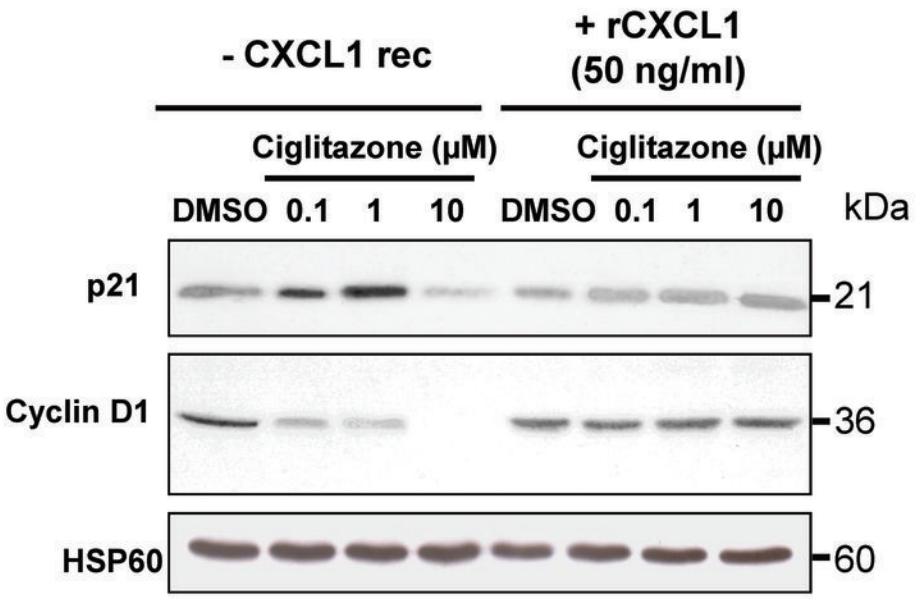

Botton *et al.*, Supplementary Figure S4

A.

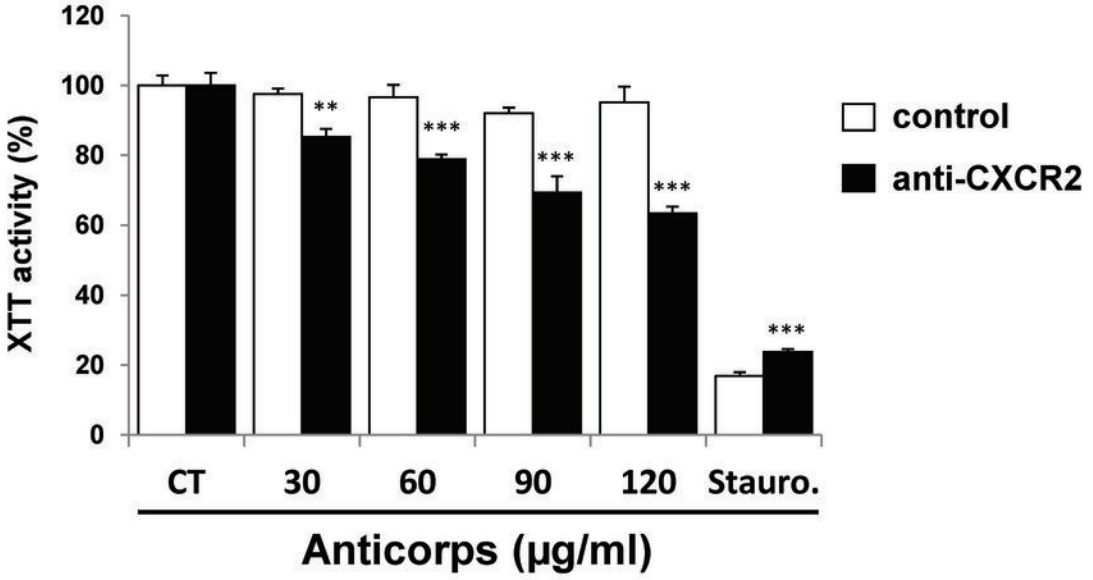

B.

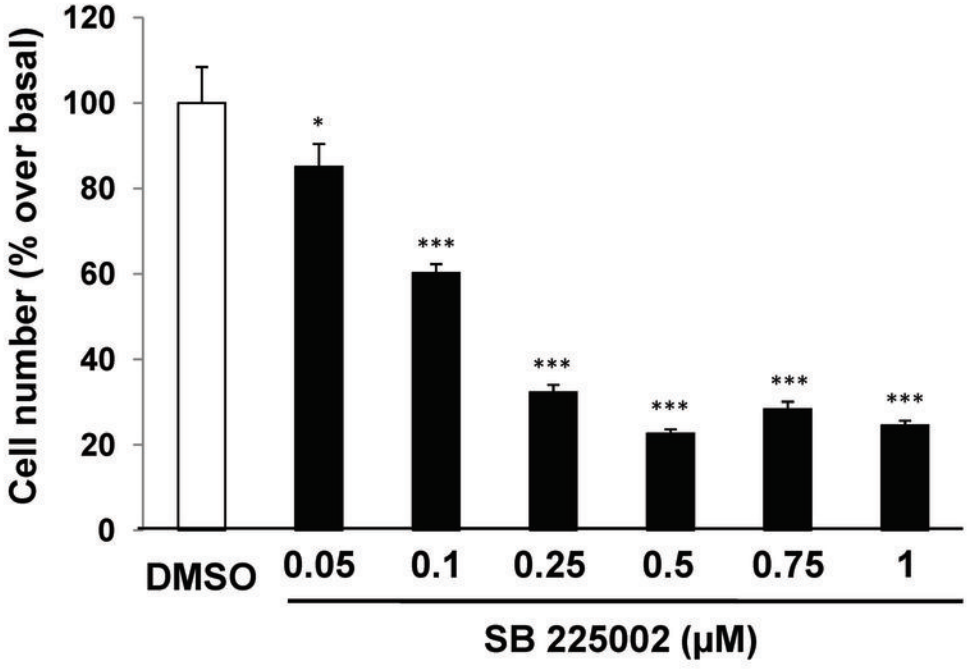

Botton *et al.*, Supplementary Figure S5